Measurement of the structure functions at HERA

- HERA colliders
- Kinematics
- Structure function definition
- The ZEUS detector
- Typical neutral current events
- Reconstruction of the kinematical variables
- Events characteristics
- Phase space
- Purity and acceptance
- Statistical and systematics uncertainties
- The structure function F_2
- Parton distributions of the proton

The HERA collider

	e-ring	p-ring
beam energies (GeV)	27,6	920
magn. bend. field (T)	0,15	5,25
dip. bend. radius (m)	610	584
max. circ. curr. (mA)	50	110
n. bunches (typical)	180	180
electron polarization	50-70%	

HERA-I
max. lumi achiev. 2.10^{31} $cm^{-2}s^{-1}$
max. yearly Lumi. deliv. 70 pb^{-1}/per expt.

HERA-II (upgrade):
Lumi: 7.5 10^{31} cm^{-2} s^{-1}
yearly Lumi 150 pb^{-1}/per expt.

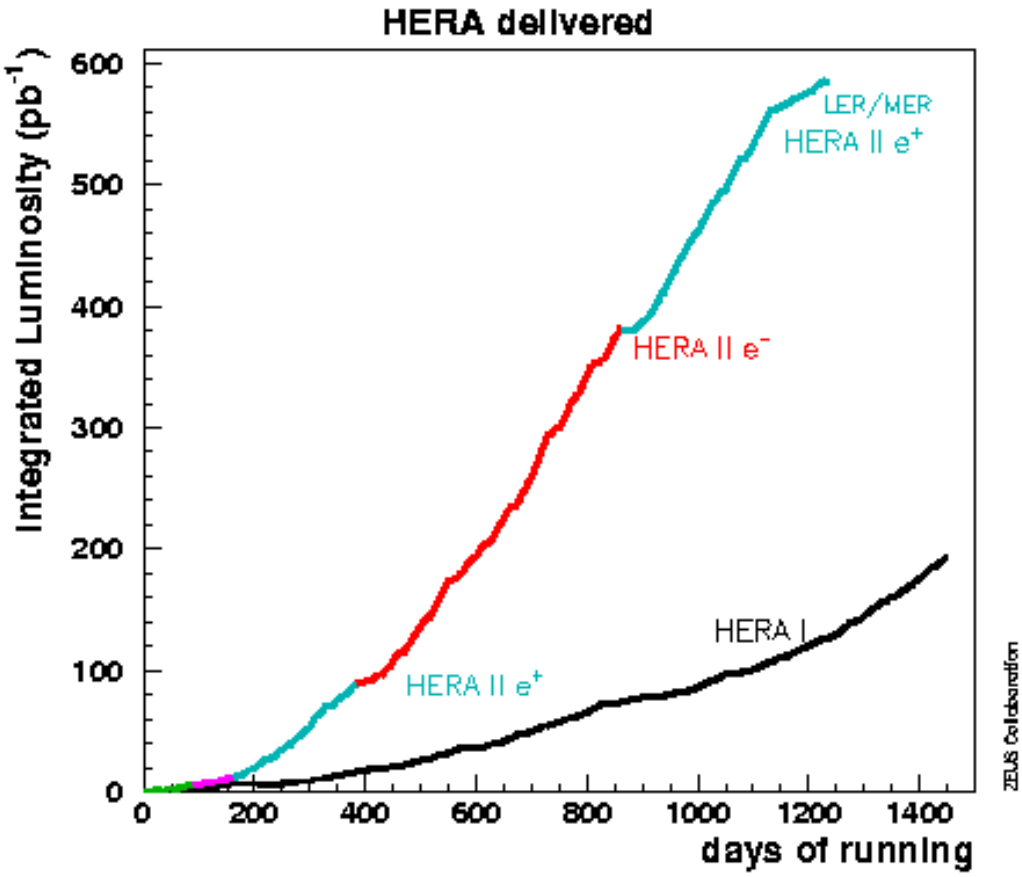

The HERA collider

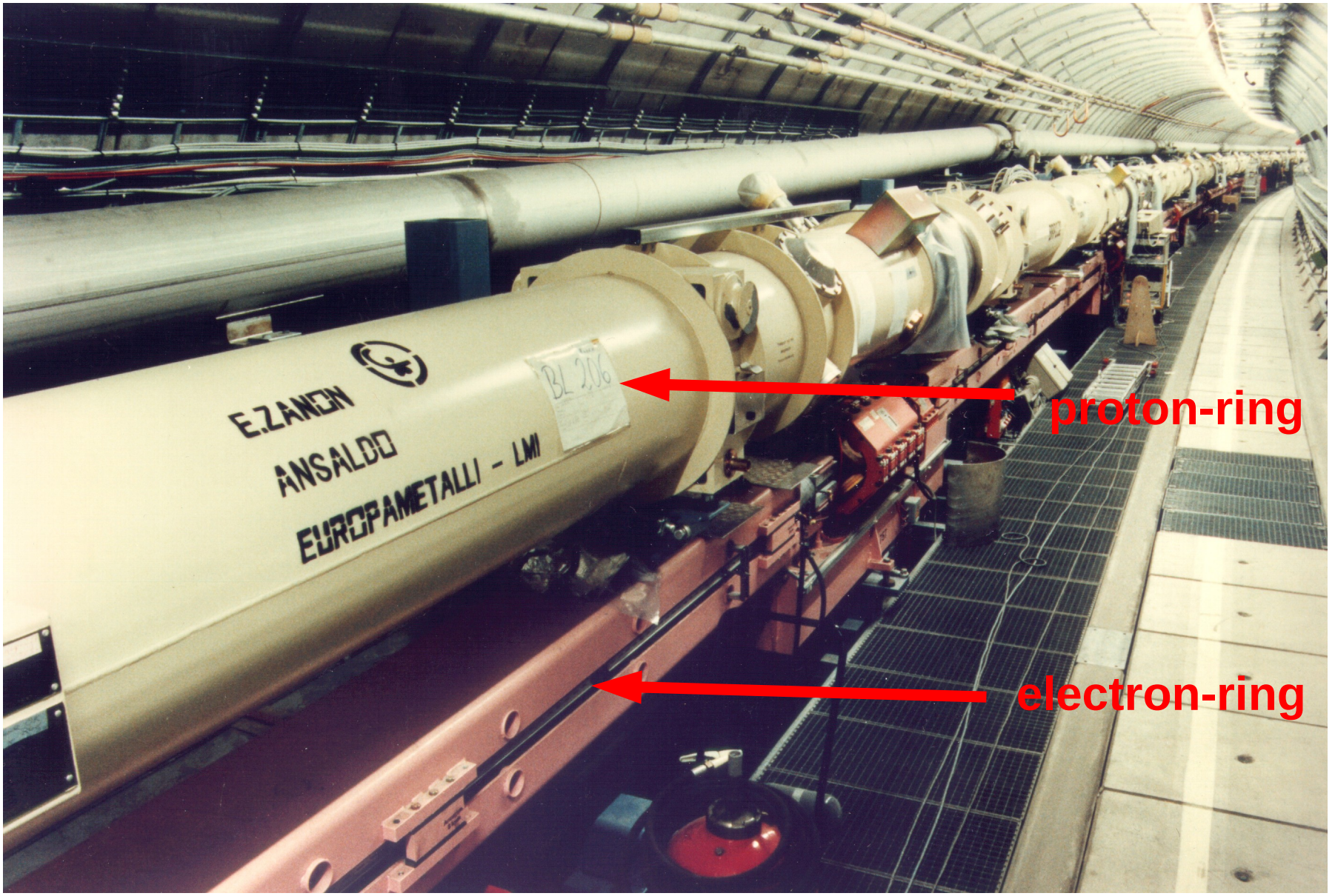

The HERA collider

spin rotator

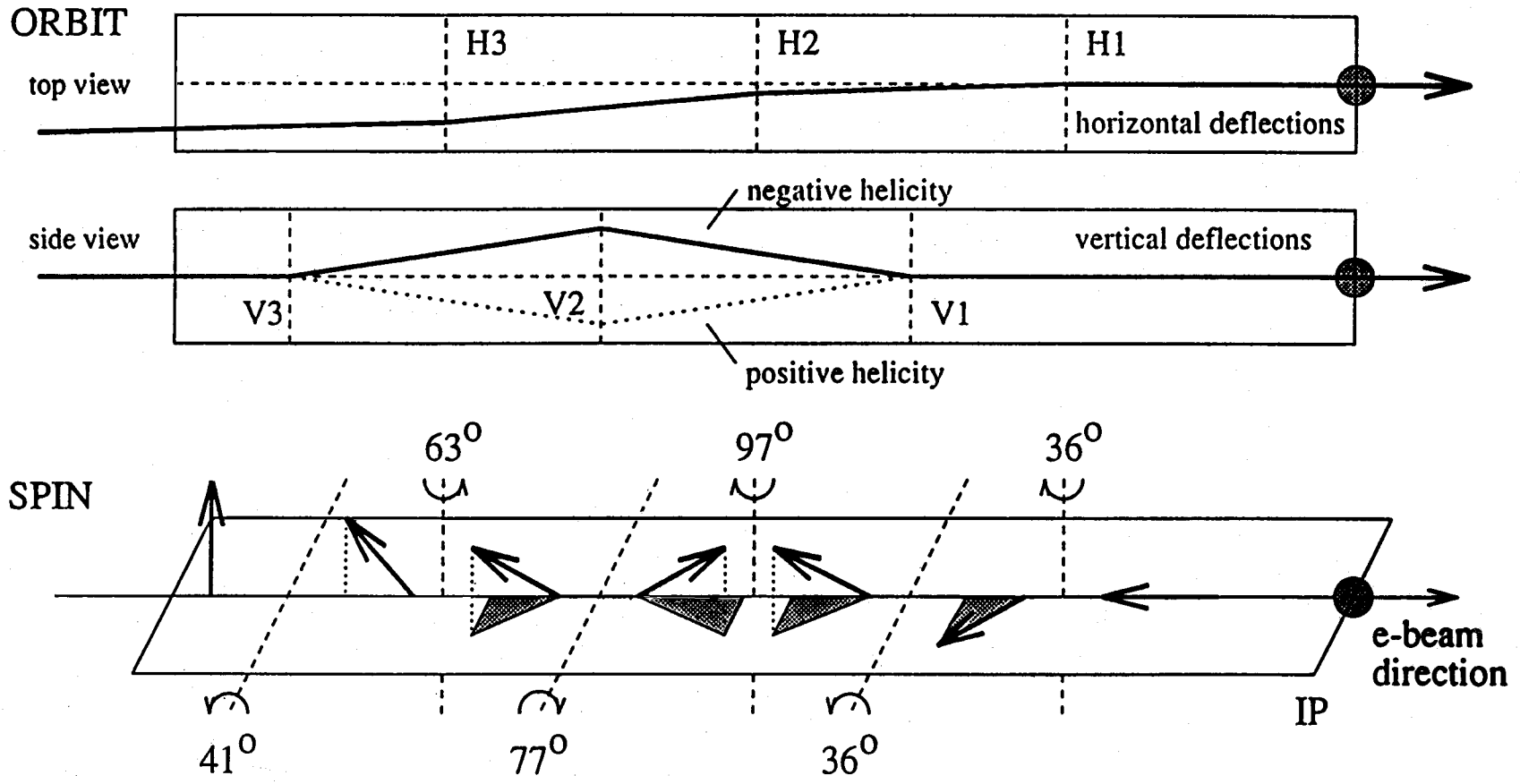

Kinematics

- The neutral current (NC) deep inelastic scattering (DIS):

$$e^{\pm} p \Rightarrow e^{\pm} X$$

can be described by the two variables: x (Bjorken) and Q^2

- The basic quantities, without QED radiation, are:

$s = (k+P)^2 = 4E_e E_p$

$Q^2 = -q^2 = -(k-k')^2$

$y = qP/kP$

$x = Q^2/2Pq$

$W^2 = (q+P)^2 = Q^2(1-x)/x + m_p^2 \approx Q^2/x$ (per $x \ll 1$)

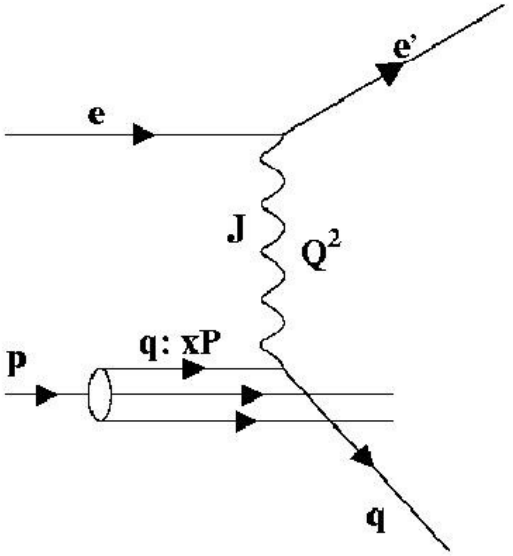

Definition of the structure functions

- The differential cross section for DIS processes can be expressed using three structure functions: F_2, F_L, xF_3

$$\frac{d^2\sigma}{dx\,dQ^2} = \frac{2\pi\alpha^2}{xQ^4}[(1+(1-y)^2)F_2 - y^2 F_L \pm (1-(1-y)^2)xF_3](1+\delta_r)$$

α = fine structure constant, δ_r = radiative corrections

The sign + (-) has to be used for the scattering of the electron (positron) against the proton.

- When F_L, xF_3 are small, negligible:

$$\frac{d^2\sigma}{dx\,dQ^2} = \frac{2\pi\alpha^2}{xQ^4}[(1+(1-y)^2)F_2](1+\delta_r)(1-\delta_L-\delta_3)$$

- F_2 includes contributes from the photon and Z^0 exchange

$$F_2 = F_2^{em}(1+\delta_z)$$

F_2^{em} represents the contribution from the photon exchange

Definition of the structure functions

- $\delta_Z = \delta_Z(x, Q^2), \delta_L = \delta_L(x, Q^2), \delta_3 = \delta_3(x, Q^2)$
- independent of the structure functions, that is indifferent to the partonic density distributions
- they are calculated using structure functions in good agreement with the data
- δ_L is usually small, except when $y \geq 0.7$ where $\delta_L \approx 0.12$
- also $\delta_{Z,3}$ are negligible for $Q^2 < 1000$ GeV^2 and small up to $Q^2 \approx 5000$ GeV^2

- In QCD, ignoring the Z^0 exchange, F_2 can be expressed in terms of the quark density of the proton:

$$F_2 = \sum e_q^2 x\, q(x, Q^2)$$

where e_q is the charge of the quark q and the sum runs over all quarks and antiquarks.

- In the partonic model: $F_L = F_2 - 2xF_1 = 0$ (Callan-Gross relation). In QCD one has : $F_L \neq 0$ (at LO where $F_L = O(\alpha_s)$)
- xF_3 is the function connected with the parity violation, very small for $Q^2 < M_Z^2$ (it is instead very important in the DIS processes with neutrinos):

$$xF_3(x, Q^2) = \sum_i B_i^o \left(xq_i(x, Q^2) - x\bar{q}_i(x, Q^2)\right)$$

B^0_i contains terms proportional to: $Q^2/(Q^2 + M_Z^2)$

The ZEUS detector

- **CTD,RTD**: central and rear tracking.
- U-scintillator **Calorimeter**:
  99.7%: solid angle coverage
  $\sigma/E = 18\%/\sqrt{E(\text{GeV})}$ for electrons
  $\sigma/E = 35\%/\sqrt{E(\text{GeV})}$ for hadrons
- **PRES**: presampler in front of FCAL and RCAL; to correct the energy of the scattered electron.
- **SRTD**: two planes of scintillator strips to measure the position of electrons scattered at low angle
- **HES**: plane of silicon pad
- **LUMI**: to measure the luminosity
- **Positron tagger**: calorimeter to measure electrons emitted at very small angles

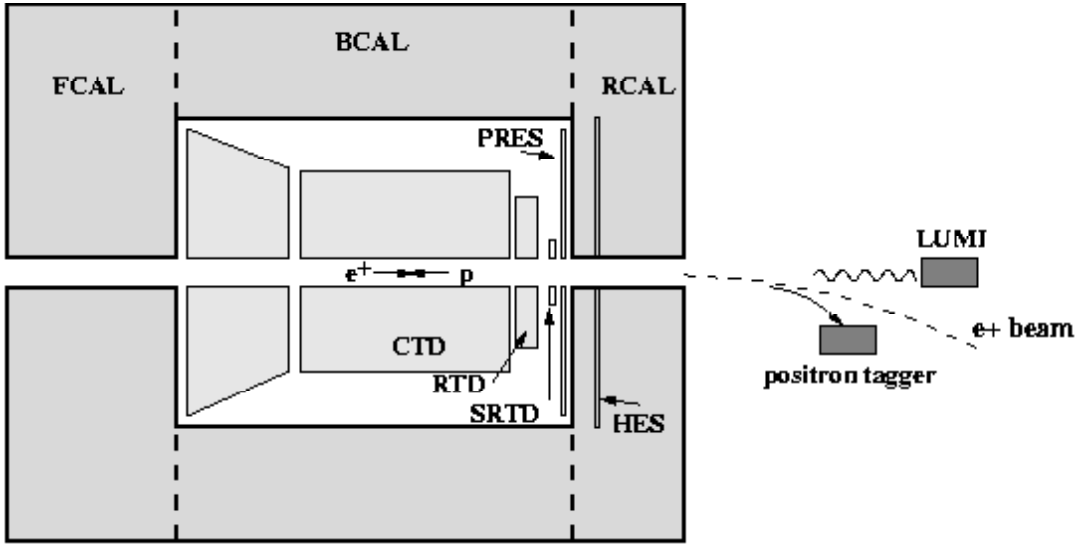

The ZEUS detector

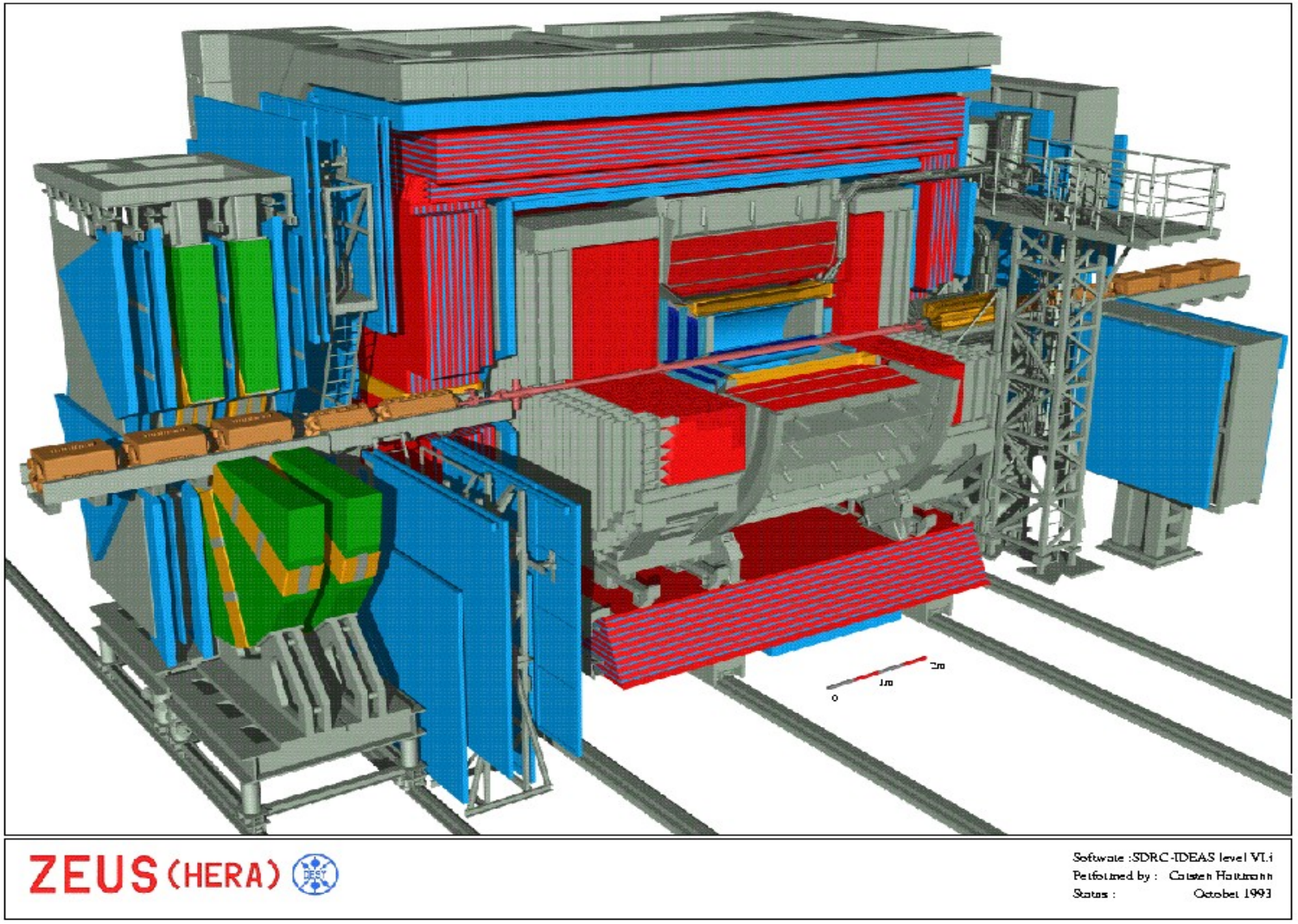

Typical Neutral Current Event

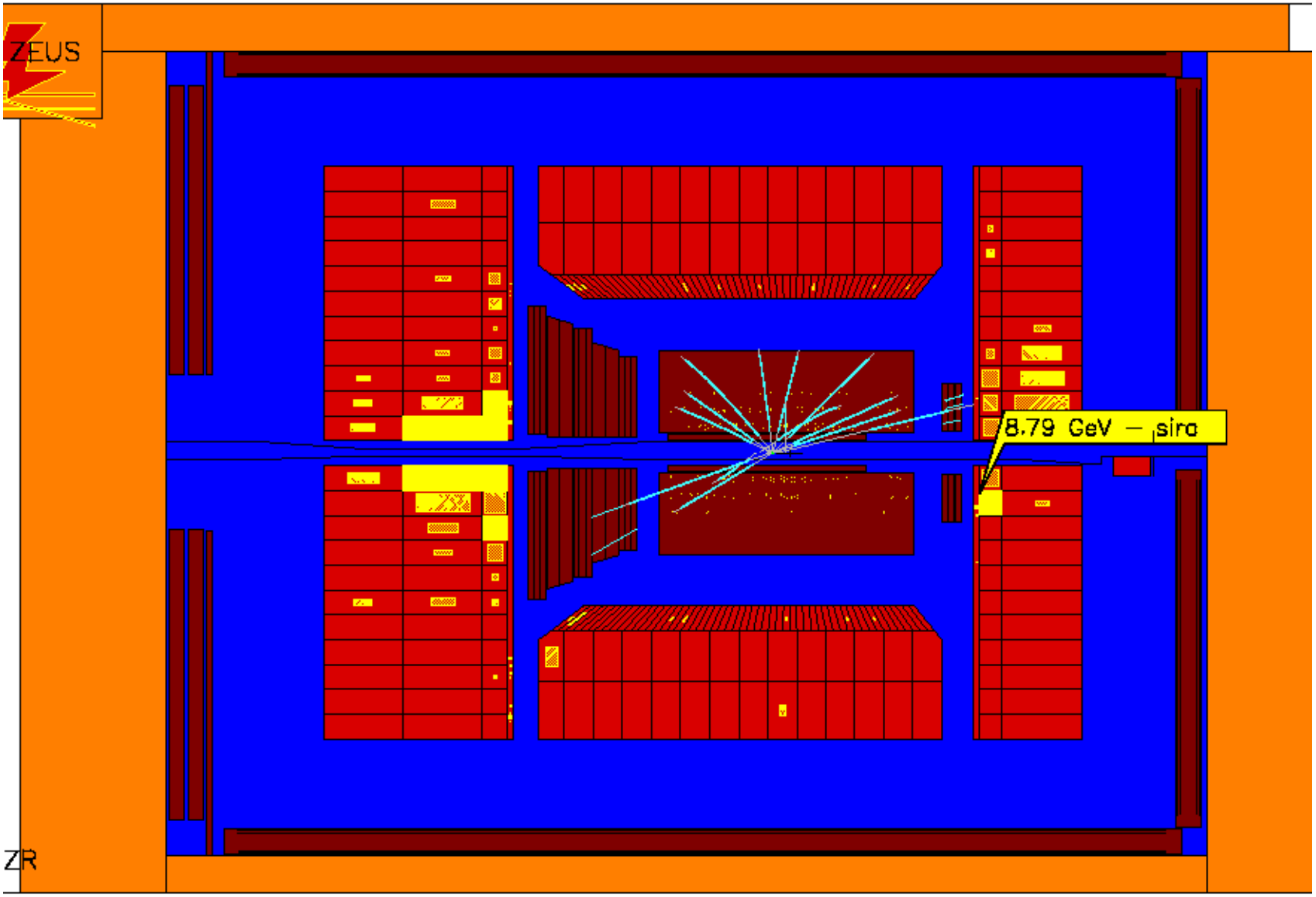

Typical Neutral Current Event

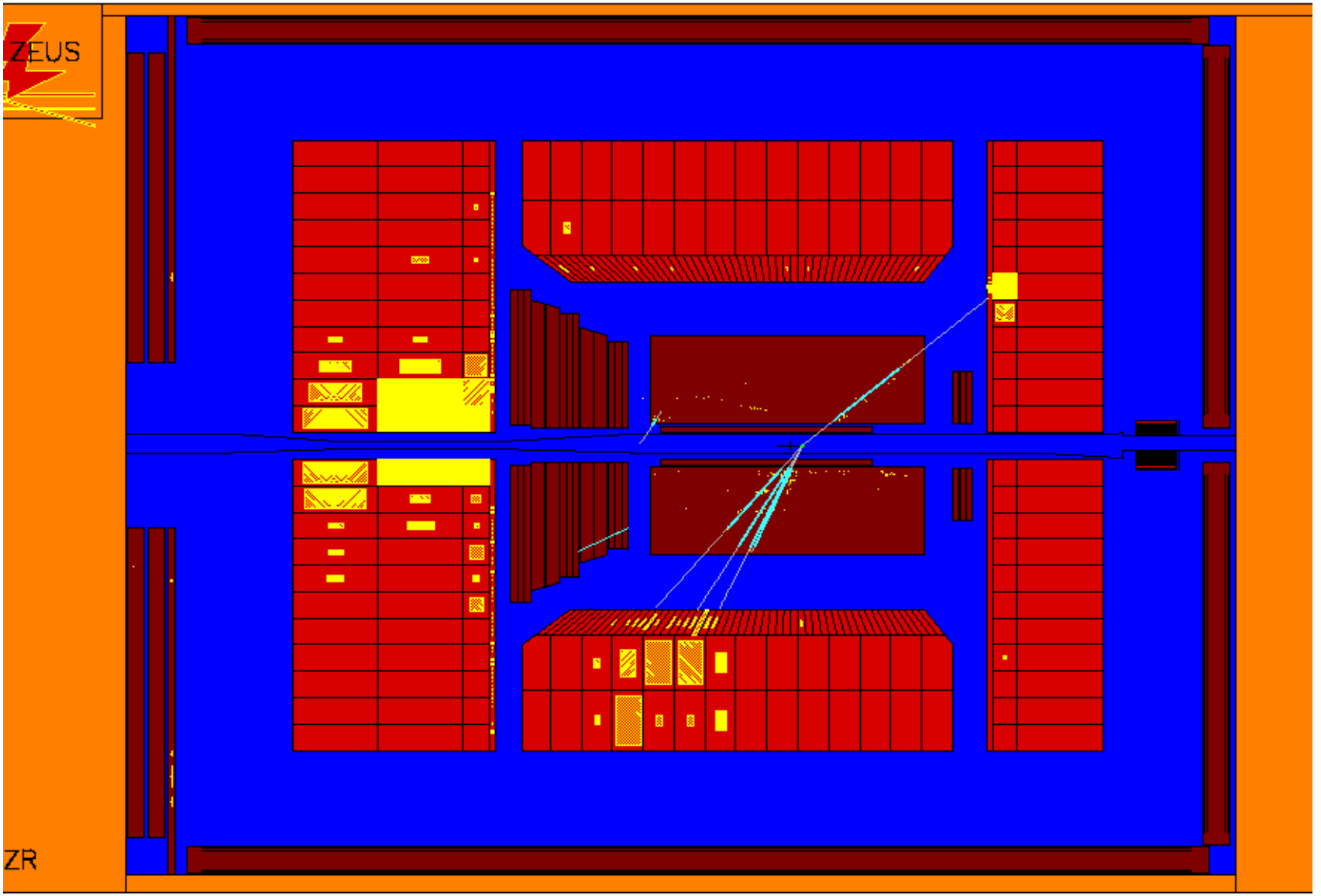

Typical Neutral Current Event

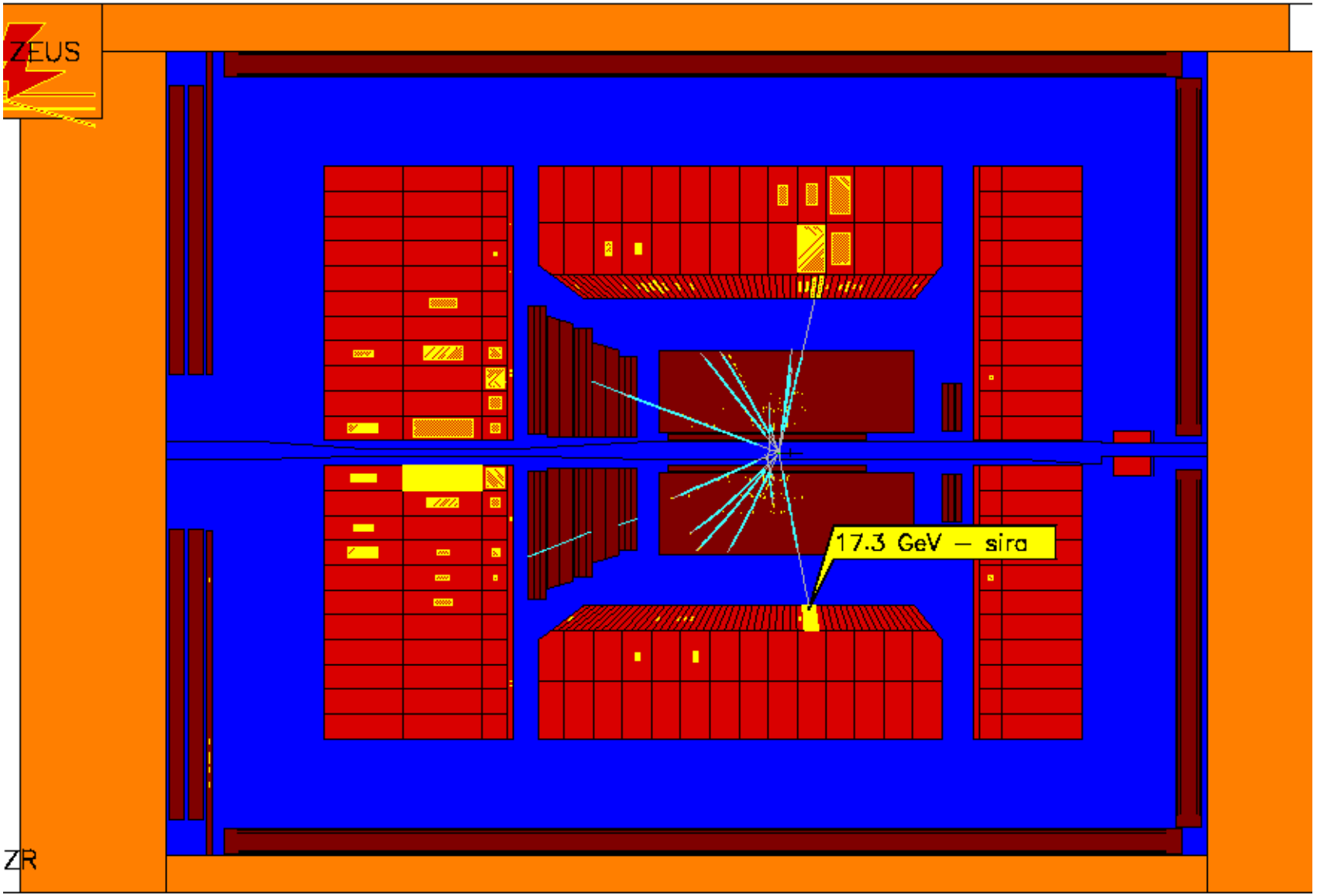

Typical Neutral Current Event

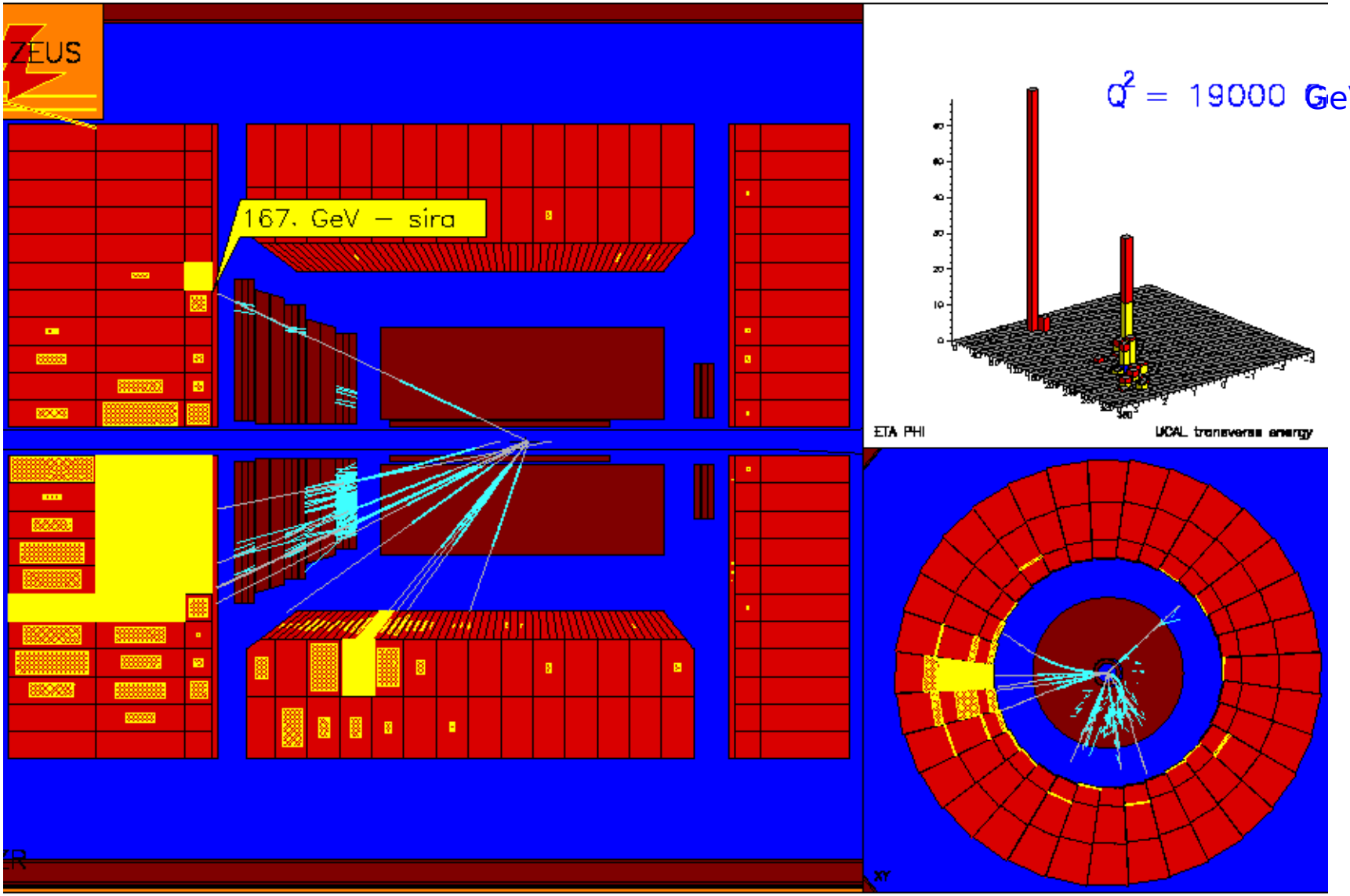

Reconstruction of the kinematical variables

- The event kinematics is determined by the following quantities:
- Energy (E'_e) and polar angle (θ_e) of the scattered electron;
- The hadronic energy is expressed through the terms of the longitudinal component:

$$\delta_h = \sum (E_h - P_{Z,h})$$

and transversal component:

$$P_{T,h} = \sqrt{\left(\sum P_{X,h}\right)^2 + \left(\sum P_{Y,h}\right)^2}$$

the sums run over all the energetic deposit not associated to the scattered electron.

- The flux of the hadronic energy is characterized by an angle γ_h:

$$\cos\gamma_h = \frac{P_{T,h}^2 - \delta_h^2}{P_{T,h}^2 + \delta_h^2}$$

- in the quark-parton model, this angle corresponds to the polar angle of the hitted quark.
- To optimize the accuracy and the precision in the variables reconstruction the following refinement are done:

$$P_{T,h} \to P_{T,e}$$
$$\delta_h \to \delta_{\Sigma,cor}$$

where $P_{T,e}$ is the transverse momentum of the scattered electron, $\delta_{\Sigma,corr} = 2E_e y_{\Sigma,corr}$ and finally:

$$\cos\gamma_{PT} = \frac{P_{T,e}^2 - \delta_{\Sigma,corr}^2}{P_{T,e}^2 + \delta_{\Sigma,corr}^2}$$

Reconstruction of the kinematical variables

- δ_h is corrected in the following manner:
  - in the regions in which δ_h is small (the hadronic system escapes forward along the beam-pipe) through MC parameterization:

$$\delta_{h,corr} = \delta_h C(P_{T,h}/P_{T,e}, \gamma_h, Q^2)$$

  - in the determination of y when δ_h is large, the information coming from the electron gives the most accurate measure:

$$y_e = 1-\left(E'_e/2E_e\right)\left(1-\cos\theta_e\right)$$

  - However, at low values of δ_h, the hadronic information gives the most accurate measure:

$$y_{corr} = \delta_{h,corr}/\left(2E_e\right)$$

  - The Σ method combines y_{corr} and y_e such that (where $\delta_e = E'_e(1-\cos\theta_e)$) :

$$y_{\Sigma,corr} = \frac{\delta_{h,corr}y_e + \delta_e y_{corr}}{\delta_e + \delta_{h,corr}}$$

Reconstruction of the kinematical variables

- At the end the kinematic variables of the event are:

$$Q^2_{PT} = 4E_e^2 \frac{\sin\gamma_{PT}(1+\cos\theta_e)}{\sin\gamma_{PT}+\sin\theta_e-\sin(\gamma_{PT}+\theta_e)}$$

$$x_{PT} = \frac{E_e}{E_p}\frac{\sin\gamma_{PT}+\sin\theta_e+\sin(\gamma_{PT}+\theta_e)}{\sin\gamma_{PT}+\sin\theta_e-\sin(\gamma_{PT}+\theta_e)}$$

$$y_{PT} = \frac{Q^2_{PT}}{s\,x_{PT}}$$

$$W^2_{PT} = Q^2_{PT}\frac{1-x_{PT}}{x_{PT}} + m_p^2$$

Events Characteristics

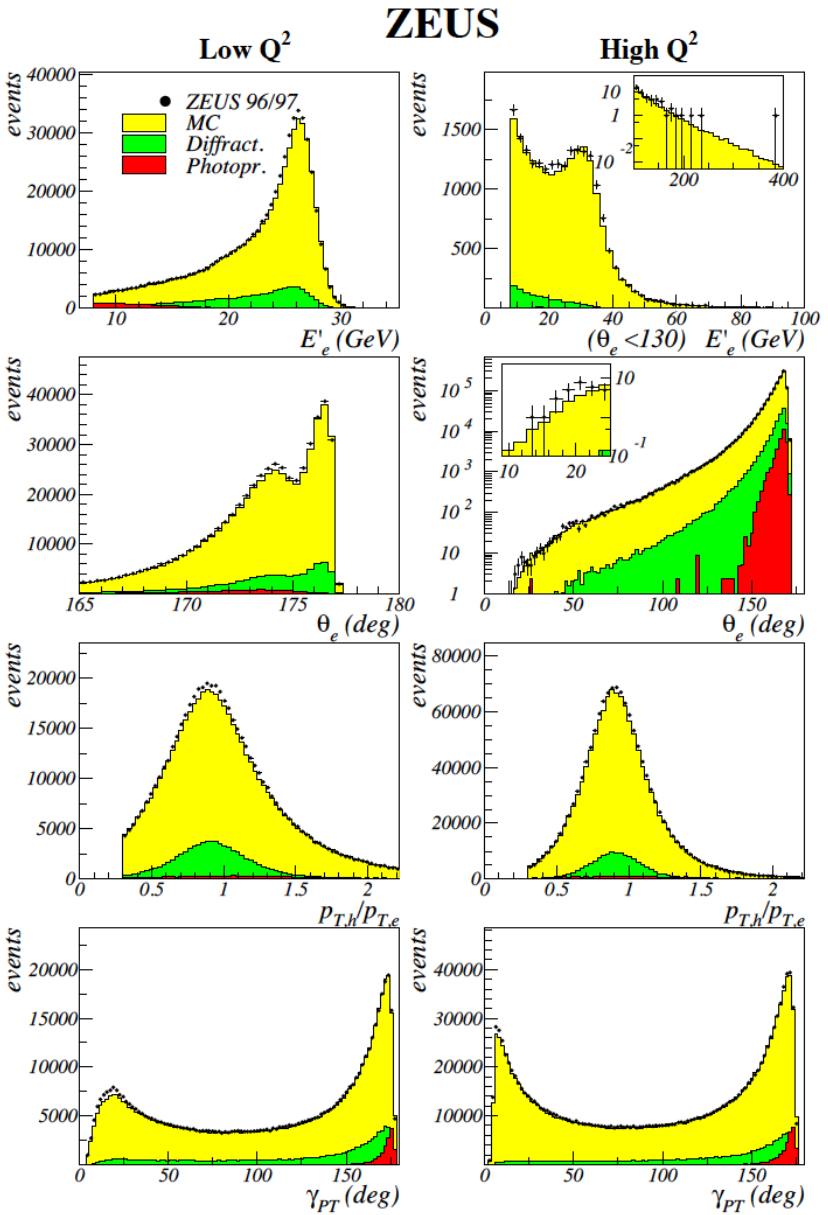

- The energy, angular and transverse momentum distribution are well reproduced by the MC simulation.
- Low Q^2: $Q^2 \geq 2$ GeV^2
- High Q^2: $Q^2 \geq 30$ GeV^2

Events Characteristics

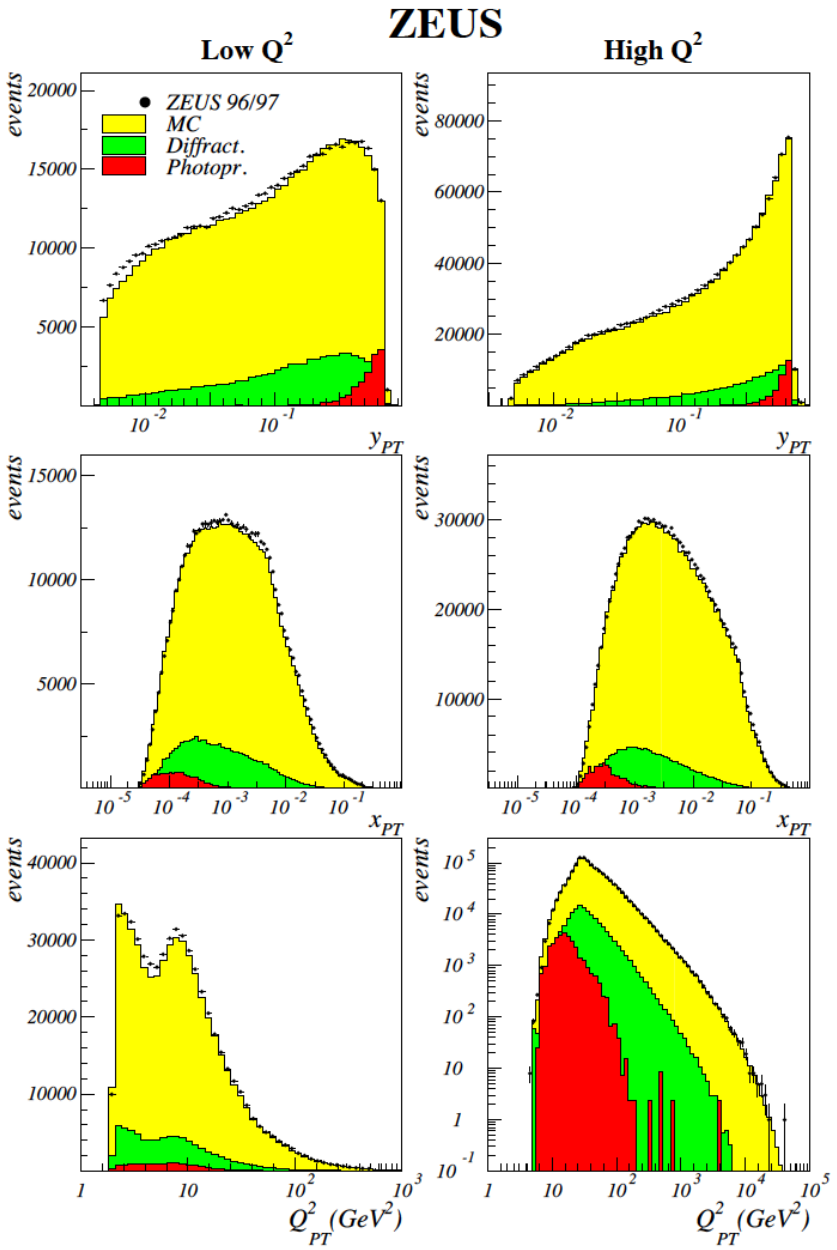

- There is a good agreement between MC and data in the region at high Q^2.
- The discrepancy at $y < 10^{-2}$ and $Q^2 < 15$ GeV^2 affect three bins in the plane (x, Q^2) respect to a total number of 242 bins. The discrepancy between data and MC is of the same order of magnitude (10%) of the systematic uncertainty.

The phase space

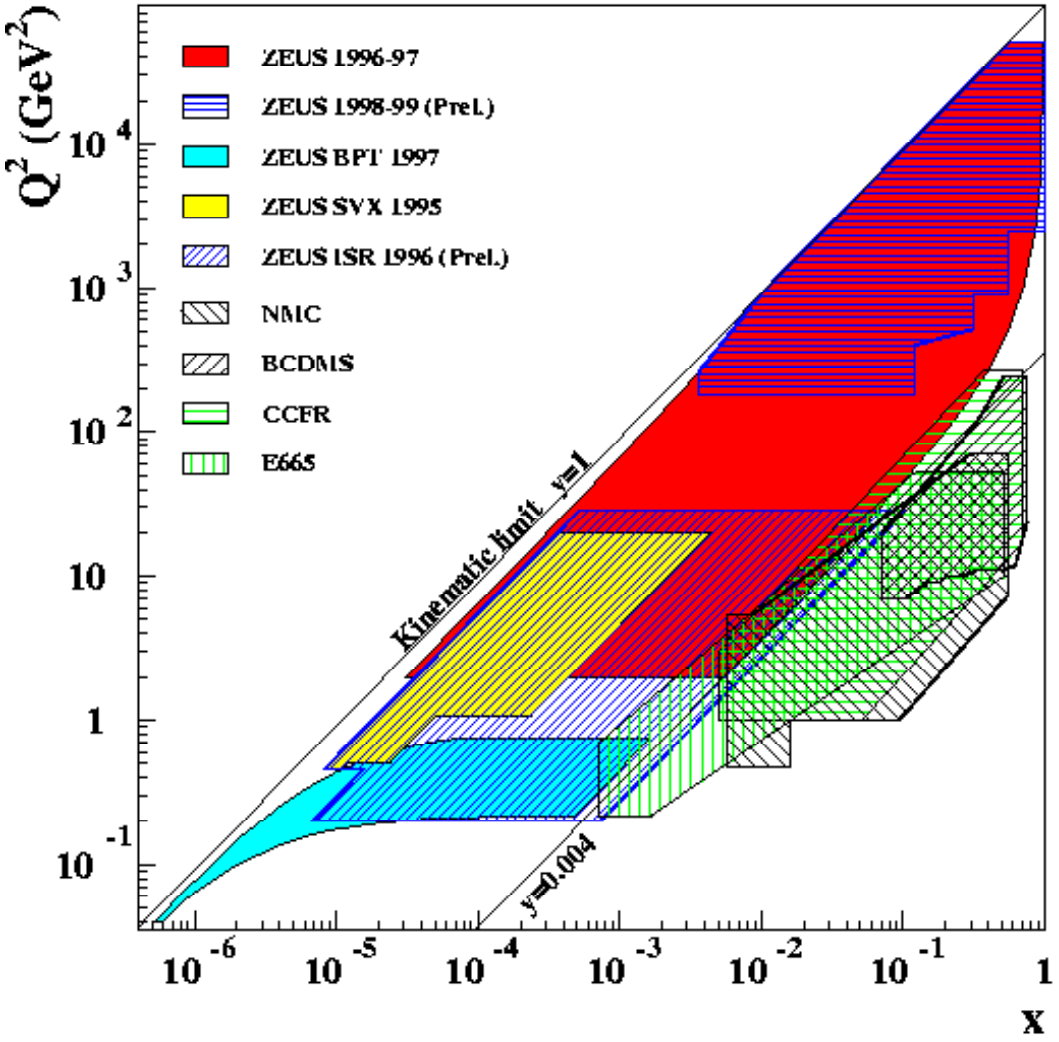

- **high *y***: sensitivity to F_L
- **low *y***: superposition with the experiments at fixed target
- **low Q^2** : transition from $\gamma^* p$ to γp
- **medium Q^2 medio**: pQCD
- **high Q^2** : electroweak studies, search for exotic phenomena

The phase space

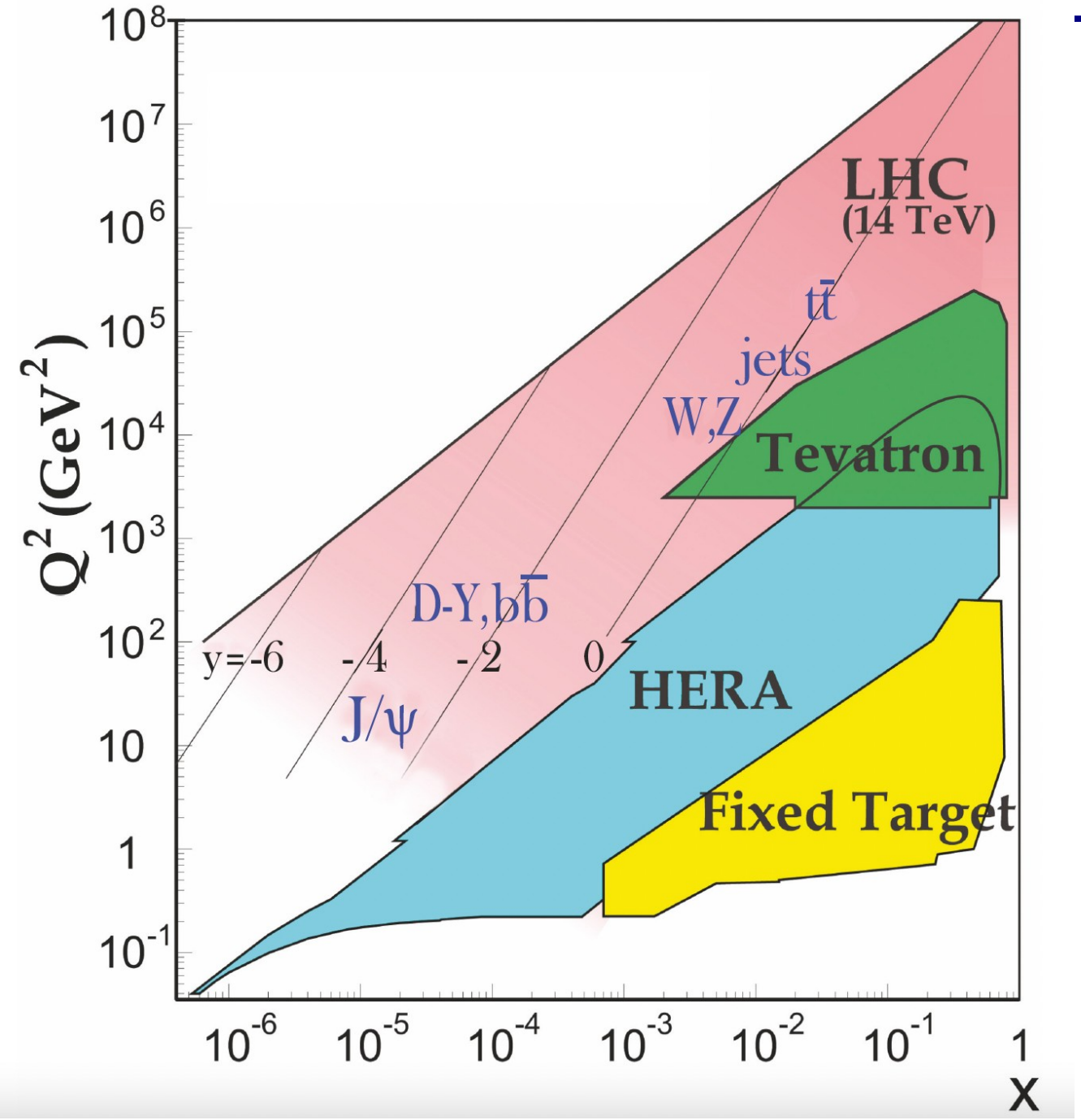

Kinematic domains in x and Q^2 probed by fixed-target and collider experiments, where Q^2 can refer either the literal Q^2 for DIS, or the hard scale of the process in hadron-hadron collision. Some of the final states accessible at LHC are indicated in the appropriate regions, whre y is the rapidity. The incoming partons have:

$$x_{1,2} = Q/14\,TeV\, e^{\pm y}$$

where Q is the hard scale of the process shown in blue in the figure.

Purity and Acceptance

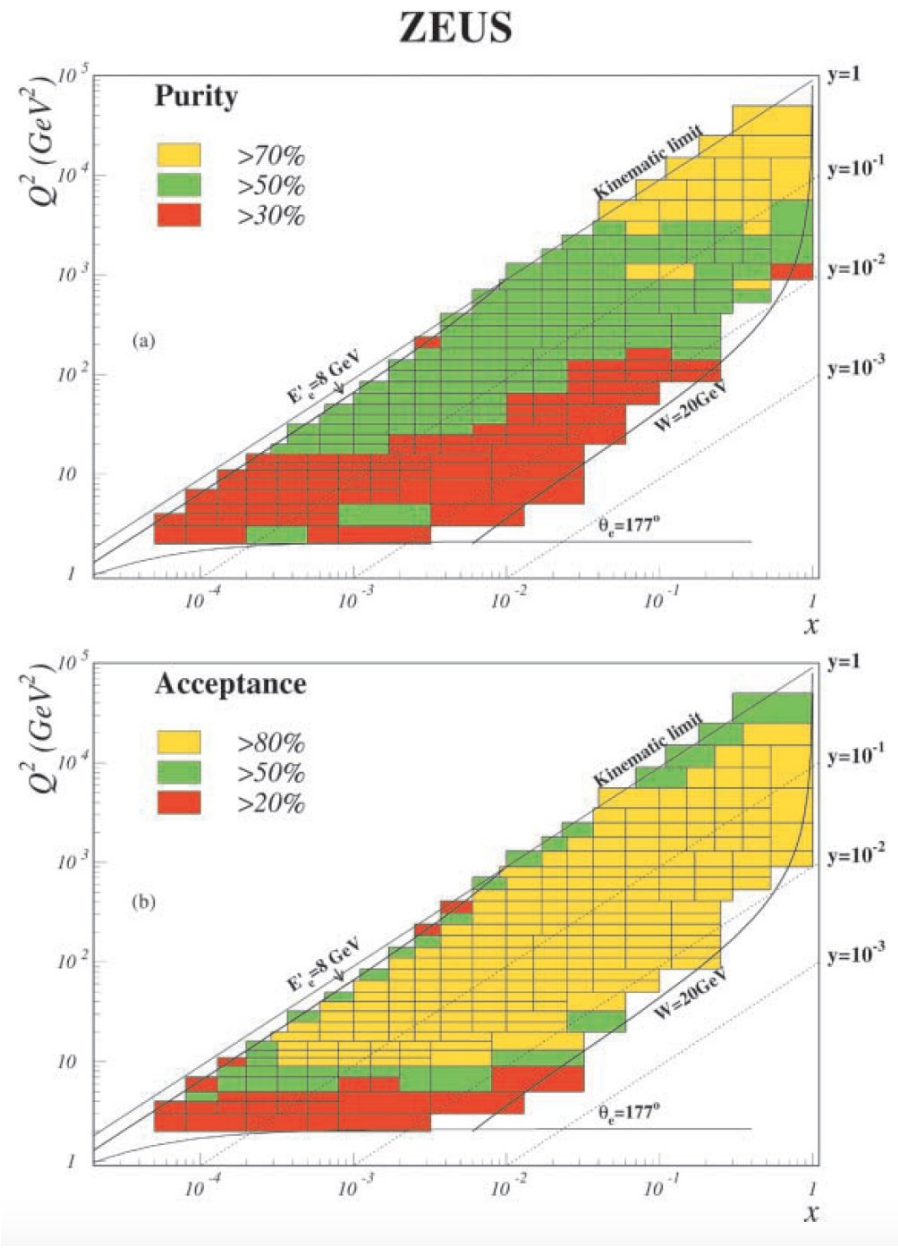

- $\delta x/x$ ~35% at $y \sim 0.005 \Rightarrow$ ~11% for $y > 0.1$
- $\delta Q^2/Q^2 \sim 2\%$ for $y \sim 0.1 \Rightarrow$ ~5% at $y \geq 0.5$ and ~10% at $y \leq 0.01$. For $Q^2 > 400$ GeV^2 $\delta Q^2/Q^2 \sim 2.5\%$.
- The dimensions of the bins are chosen following the resolution. At high Q^2 and also at low y the dimensions are larger to take into account the low statistics.
- Each bin has to have $A > 20\%$ and $P > 30\%$.
- ***Acceptance*** = (n. rec. evt && gen.in the bin)/ (n. evt. gen. in the bin)
  Purity = (n. evt. gen.in the bin)&&(n. evt. rec. in the bin)/(n. evt. rec. in the bin)

Statistical and Systematical Uncertainties

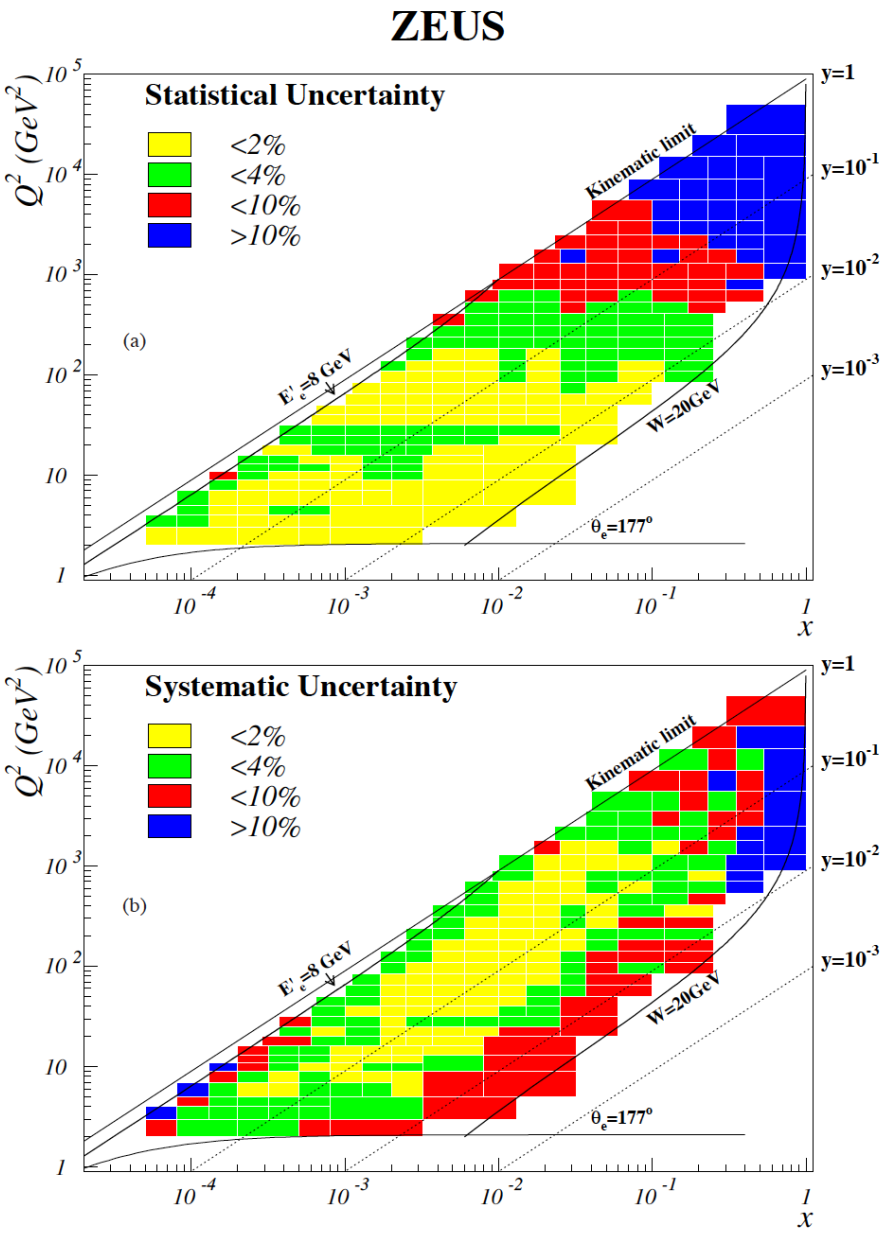

- Over a large part of the phase space both the statistical and systematic uncertainties are < 2%.
- Along the edge of the phase space the systematic uncertainties grow to ~ 10%. For $y \geq 0.5$ due to the uncertainty of the photoproduction background; for $y \leq 0.01$ due to the uncertainties in the hadronic energetic flux.

The structure function F_2

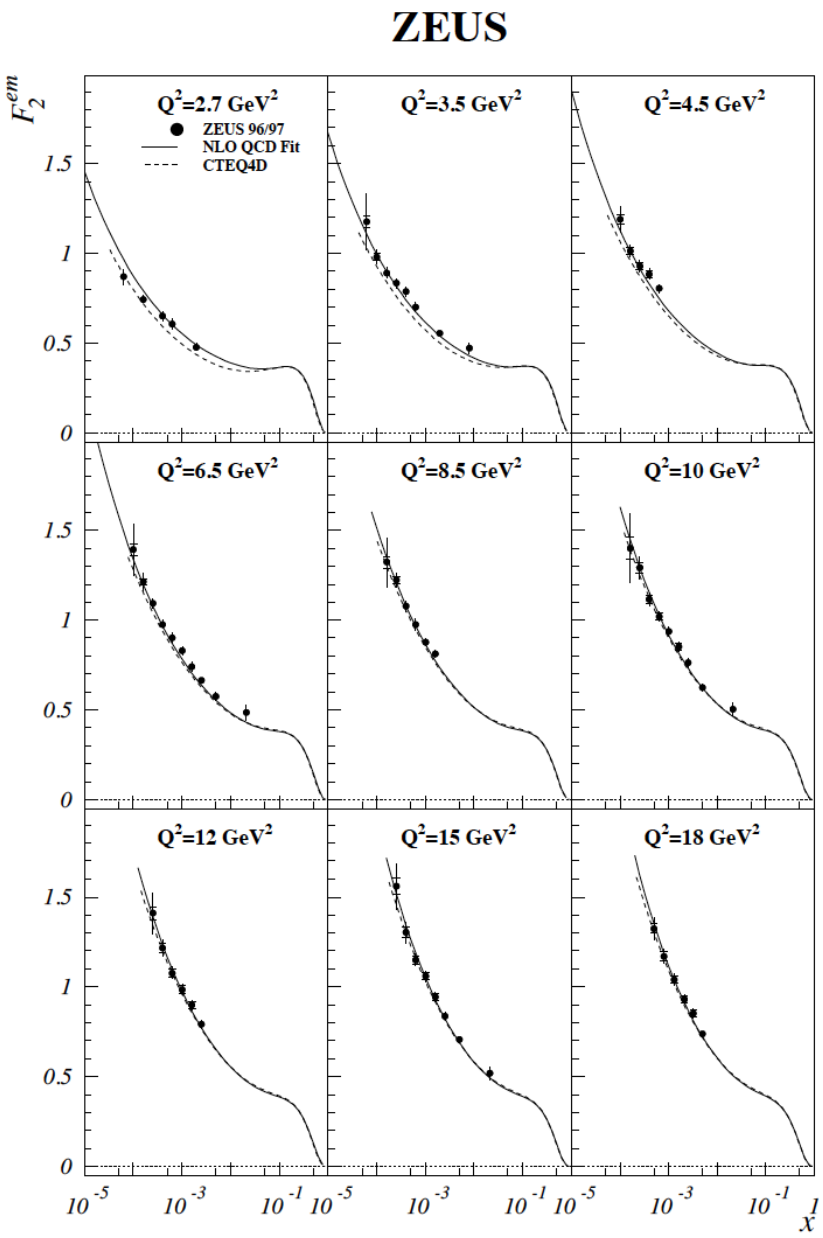

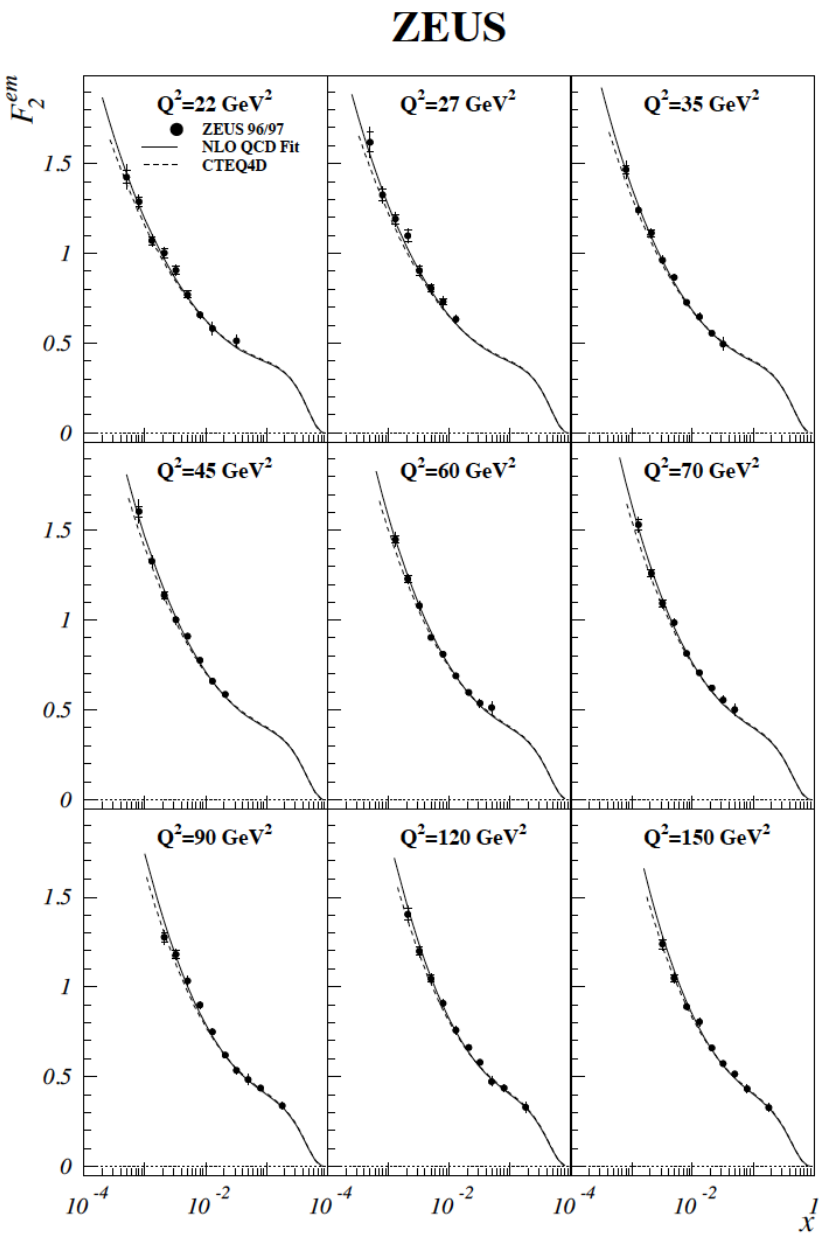

The structure function F_2

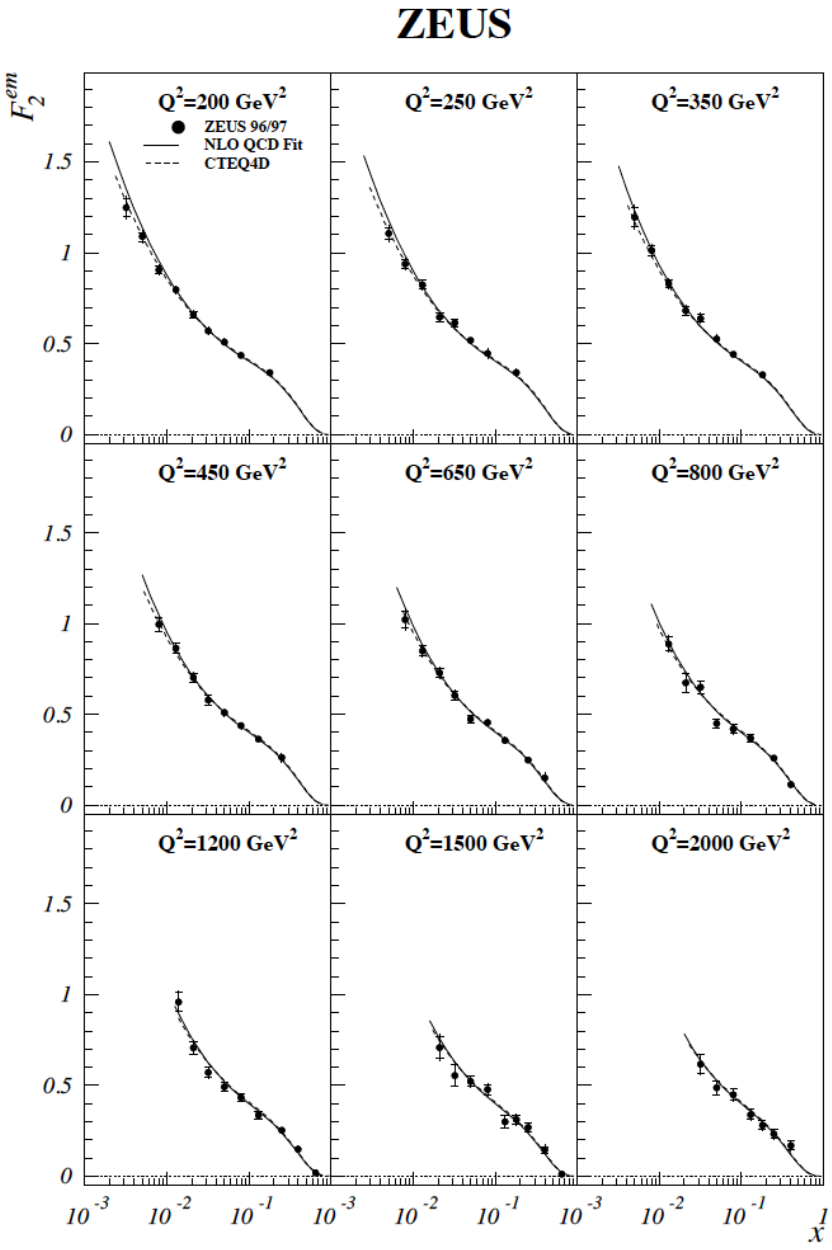

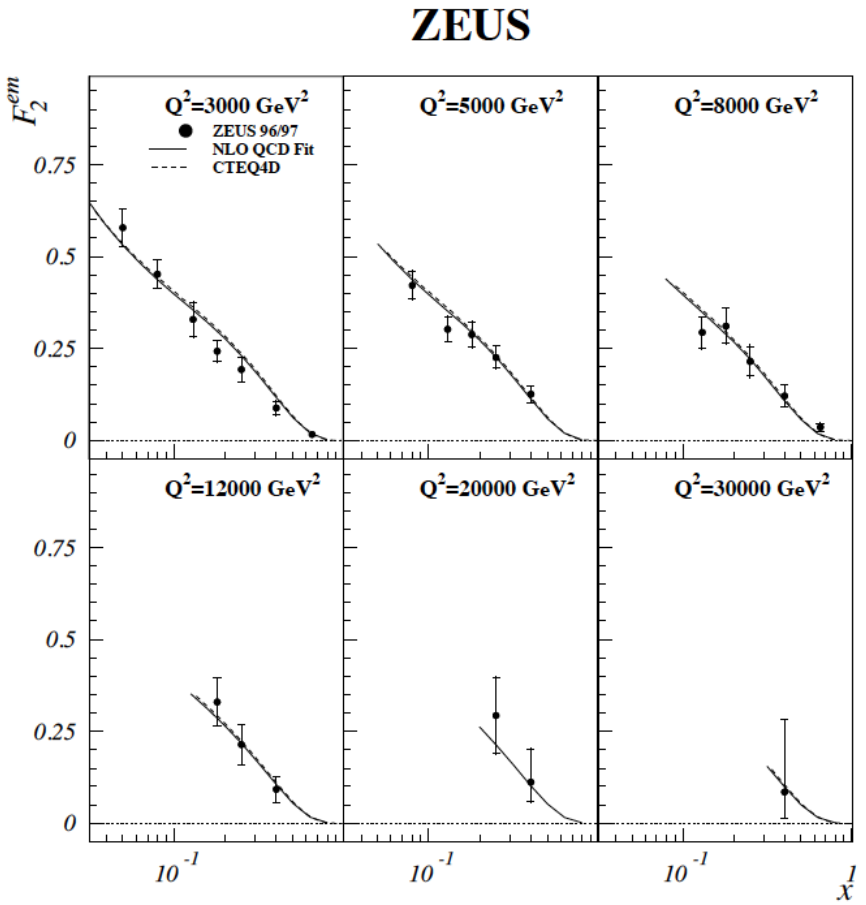

The structure function F_2

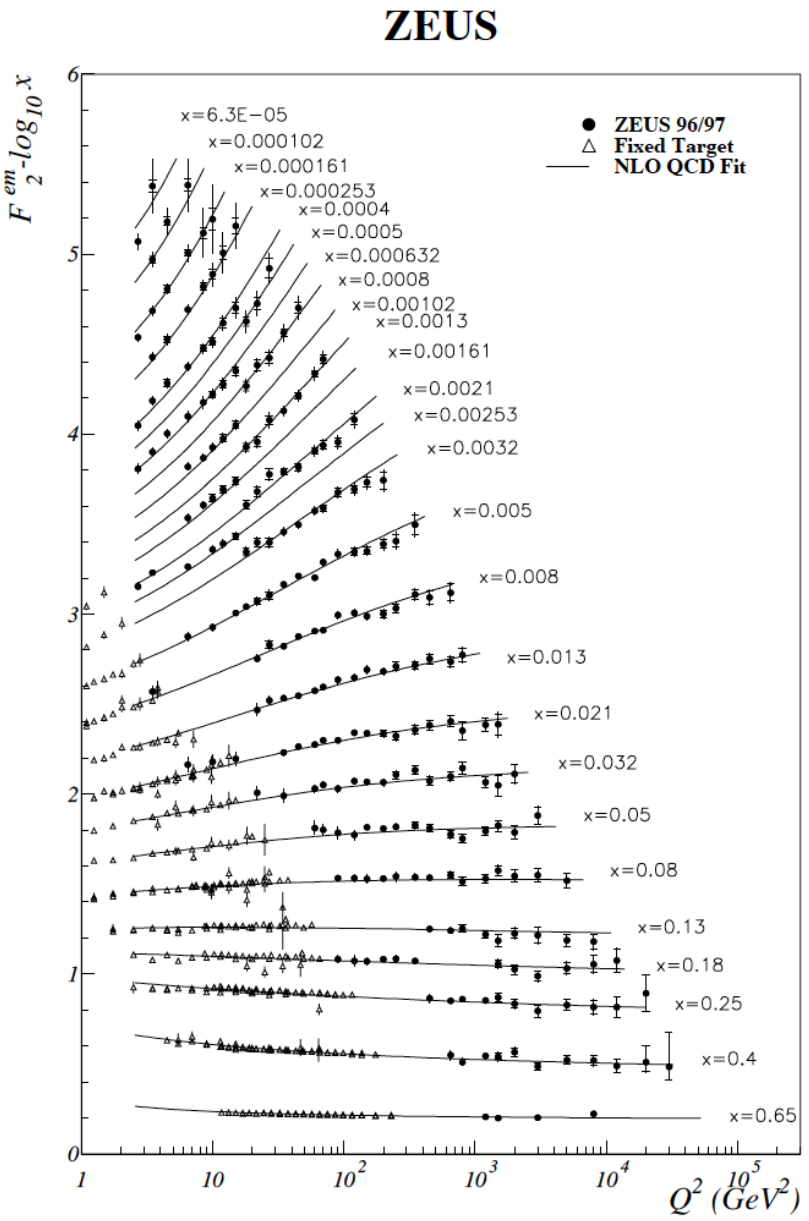

- The **scaling violations** are very clear, they diminish growing x.
- There is a good agreement between ZEUS data and data from fixed target experiments at high x, where they superimpose.
- The data cover 4 orders of magnitude in Q^2

Parton Distributions in the proton

General receipt for the determination of the p.d.f.

1) A particular analytic form of the p.d.f. is taken as valid at a certain starting value of $Q^2 = Q^2_0$
2) The value of Q^2_0 is arbitrary, but high enough such that $\alpha_s(Q^2_0)$ is sufficiently small to make pQCD applicable
3) The DGLAP equations are used to evolve the p.d.f. to a different Q^2
4) The p.d.f. are convoluted with the splitting functions, suitable to the chosen renormalization scheme, in order to make predictions for the structure functions.
5) These predictions are then fitted to the data: typically the χ^2 fit uses between 10 to 20 parameters in order to describe 1500-2000 data points distributed along the (x,Q^2) plane.
6) The fit parameters are those necessary to determine the initial analytic form and $\alpha_s(M_z^2)$ (or Λ_{QCD})

Parton Distributions in the proton

General comments:

1) If a good χ^2 is obtained:
   - stringent test of the pQCD validity within the DGLAP formalism
   - a method to determine the p.d.f.
   - and the value of $\alpha_s(M_z^2)$

2) The initial analytic form of the p.d.f. is valid only for Q^2_0. The p.d.f. are evaluated through the DGLAP equations at different values of Q^2. The p.d.f. evaluated by the fit are given in a (x,Q^2) grid, through interpolation the p.d.f. are evaluated on any (x,Q^2) point.

3) p.d.f. in the market:
   - from theoretical groups (main care concentrated in the estimation of the uncertainties coming from the theoretical structure and from the assumption of the input model):
     - MRST
     - CTEQ
     - GRV
     - NNPDF
     - ABMP
   - from experimental groups (main care concentrated in the estimation of the uncertainties coming from the experimental uncertainties):
     - ZEUS, H1 (HERAPDF)
     - ATLAS, CMS

Parton Distributions in the proton

The problem of the data sets

1) **In general it is preferred to use data sets from experiments using hydrogen or deuterium targets.** The data from DIS experiments using heavy target have to pass through various corrections before to be used:
   - nuclear shadowing;
   - binding energies effects;
   - effects due to the Fermi motion

2) However data from experiments using ν beams on heavy targets are used because they help to constrain the p.d.f. of the valence quarks. (CCFR experiment at Fermilab)

3) To have measures of good precision it is necessary to correct also the deuterium data.

4) Uncertainties on these corrections produce other uncertainties on the ratio d_v/u_v at high x.

5) In order to have a good χ^2 fit , the data sets have to be consistent between them.

Parton Distributions in the proton

The problem of the data sets

List of the data sets usually used (but see also the last slides) :

Beam	Targets	Experiment	$Q^2(GeV^2)$	x	R	Process
e^-	p,d,A	SLAC	0.6-30	0.06-0.9	✔	NC
μ	p,d,A	BCDMS	7 – 260	0.06 – 0.8	✔	NC
μ	p,d,A	NMC	0.5 – 75	0.0045 – 0.6	✔	NC
μ	p,d,A	E665	0.2 – 75	$8 \cdot 10^{-4}$ – 0.6	–	NC
ν	Fe	CCFR	1 -500	0.015 – 0.65	✔	CC
$e^{\pm}$, p	–	H1	0.35 – $3 \cdot 10^5$	$6 \cdot 10^{-6}$ – 0.65	✔	NC,CC
$e^{\pm}$, p	–	ZEUS	0.045 – $3 \cdot 10^5$	$6 \cdot 10^{-7}$ – 0.65	–	NC,CC

R = $\sigma_L/\sigma_T = F_L/(F_2-F_L)$ ... ignoring the mass terms

Parton Distributions in the proton

New strategy used by ZEUS:

1) **Only the ZEUS data are used:**
   - **there are no problems of normalization between different experiments;**
   - **the treatment of the systematics uncertainties is more reliable;**
   - **there are no uncertainties coming from the correction of the data from heavy target;**
   - **no higher twist** (*higher twist* = technical term for the $1/Q^2$ corrections to the leading expressions of the structure functions; these contributions are not well known and are important at high x and low Q^2 , that is at low W)
   - **there are no assumptions on the isospin symmetry**

2) As we will see the precision of the p.d.f. obtained by ZEUS in this manner is limited by the statistical uncertainties (in principle they can be reduced using more data, for example using HERAII data), instead the precisions of the p.d.f. obtained through global fits are limited by the systematic uncertainties of the chosen experiments (difficult to diminish).

3) This strategy was married by the H1 collaboration. Now the two HERA experiments have combined all their useful data (HERAPDF see later).

Parton Distributions in the proton

ZEUS Data sets: NC $e^{\pm}p$ scattering

$$\frac{d^2\sigma^{NC}(e^{\pm}p)}{dxdQ^2} = \frac{2\pi\alpha^2}{xQ^4}\left[Y_- F_2(x,Q^2) - y^2 F_L(x,Q^2) \mp Y_+ xF_3(x,Q^2)\right]$$

$$Y_{\pm} = 1 \pm (1-y^2)$$

- F_2 e xF_3 are directly connected with the quarks distribution and their Q^2 dependence, scaling violation, is predicted by QCD:
  - At $Q^2 \lesssim 1000$ GeV^2, the photon exchange dominates, and so also F_2
  - For $x \lesssim 10^{-2}$, F_2 is dominated by the sea quarks (its Q^2 dependence is driven by the gluons)
  - At high Q^2 xF_3 becomes more and more important; it gives information about the p.d.f. of the valence quarks.
- F_L is important only at high y

Parton Distributions in the proton

ZEUS Data sets: CC $e^{\pm}p$ scattering

$$\frac{d^2\sigma^{CC}(e^+p)}{dx\,dQ^2} = \frac{G_F^2 M_W^4}{2\pi x\,(Q^2+M_W^2)^2}\,x\,[(\bar{u}+\bar{c})+(1-y)^2(d+s)]$$

$$\frac{d^2\sigma^{CC}(e^-p)}{dx\,dQ^2} = \frac{G_F^2 M_W^4}{2\pi x\,(Q^2+M_W^2)^2}\,x\,[(u+c)+(1-y)^2(\bar{d}+\bar{s})]$$

- e^-p CC gives information on the valence U quarks at high x
- e^+p CC gives information on the valence D quarks at high x

Parton Distributions in the proton

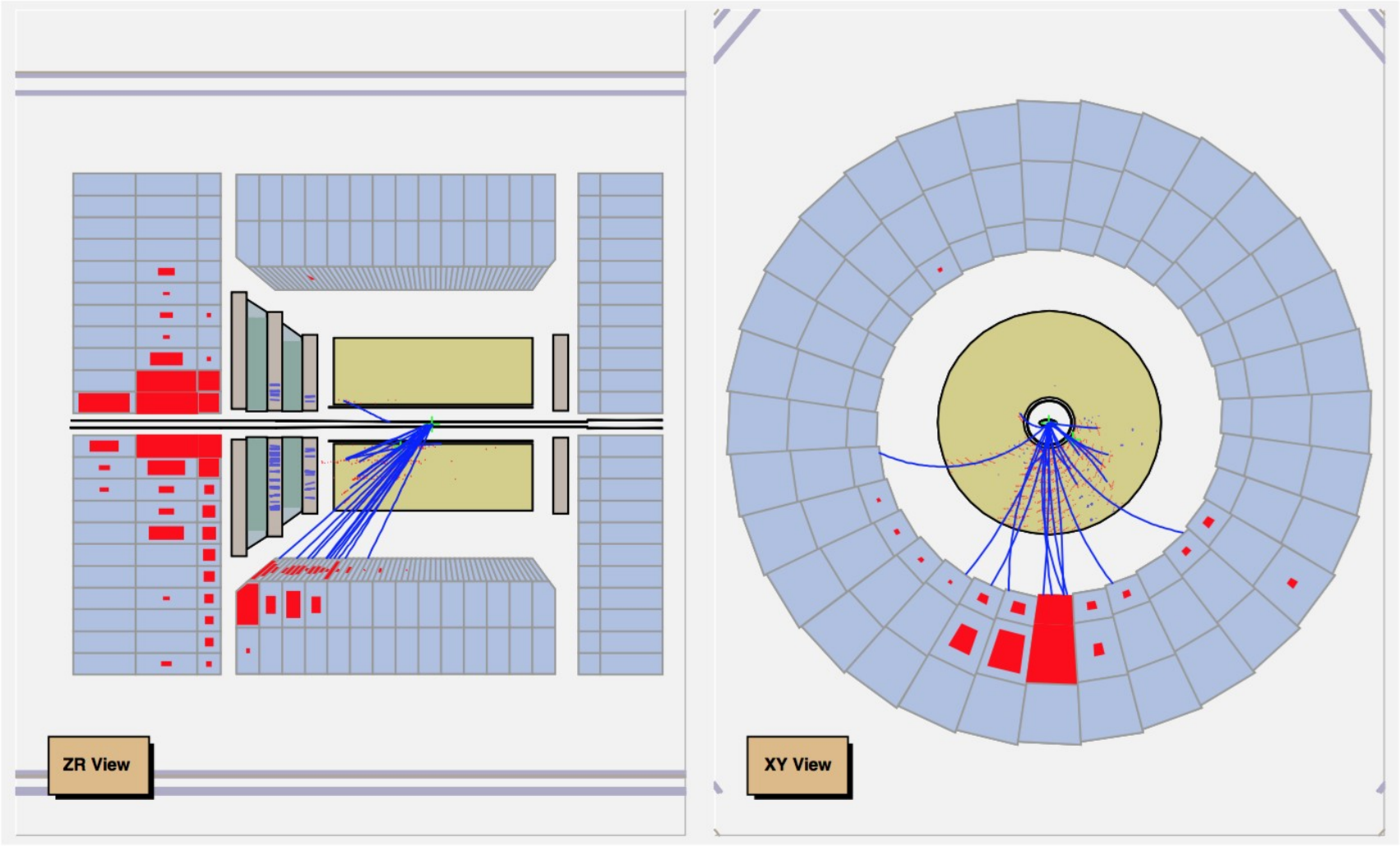

Figure A.1: Visualized CC event number 13581 of run 33423 with the reconstructed kinematic variables $Q^2 = 1517\,\mathrm{GeV}^2$, $x = 0.061$, $y = 0.245$, $\gamma_\mathrm{h} = 0.76$ rad.

Parton Distributions in the proton

ZEUS Data sets: production of jet in e^+p and of dijet in γp

The inclusive cross sections depend directly on the p.d.f. of the quarks, the p.d.f. of the gluons affect only indirectly through the **scaling violation**.

$$\frac{d\, q_i(x, Q^2)}{d \ln Q^2} = \frac{\alpha_s(Q^2)}{2\pi} \int_x^1 \left[\sum_j q_j(y, Q^2) P_{q_i q_j}\left(\frac{x}{y}\right) + g(y, Q^2) P_{q_i g}\left(\frac{x}{y}\right) \right]$$

The p.d.f. of the gluons can be obtained by the scaling violation. The shape of the p.d.f. of the gluons and the value of $\alpha_s(M_Z)$ are correlated through the DGLAP equations.

The QCD processes giving origin to the scaling violation (**QCD-Compton** (QCDC) and **boson-gluon-fusion** (BGF)) are characterized by **jets** in the final state.

Parton Distributions in the proton

ZEUS Data sets: production of jet in e^+p and of dijet in γp

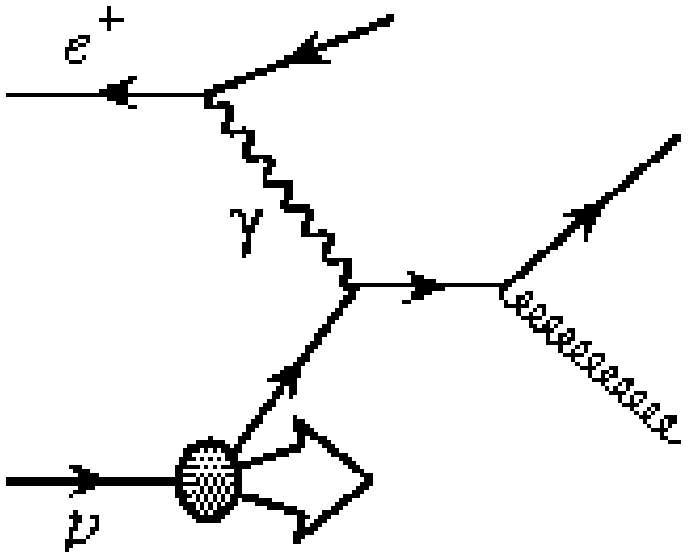

QCDC: the cross section depends on $\alpha_s(M_Z)$ and on the p.d.f. of the quarks. QCDC dominates at high energy scales; being known the p.d.f. of the quarks, the value of $\alpha_s(M_Z)$ can be extracted without strong correlation with the shape of the gluons.

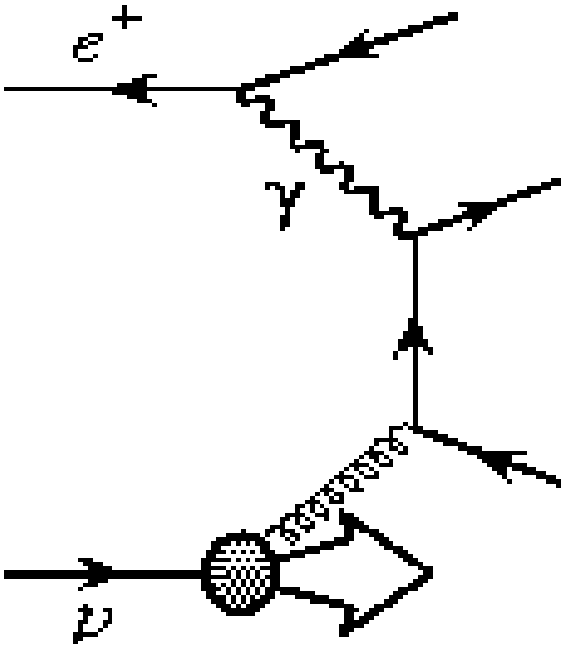

BGF: the cross section depends on $\alpha_s(M_Z)$ and on the p.d.f. of the gluons for $0.01 \lesssim x \lesssim 0.4$

Parton Distributions in the proton

- ZEUS parameterizes the p.d.f. at a given Q^2_0 in this manner:

$$xf(x) = p_1 x^{p_2}(1-x)^{p_3}(1+p_4 x)$$

for x $\Rightarrow$ 0 the distributions go to zero or are singular, for x $\Rightarrow$1 they go to 0

Parton Distributions in the proton

- The parametirezed p.d.f. are:

$$xu_v(x) = x(u - \bar{u})$$
$$xd_v(x) = x(d - \bar{d})$$
$$x\Delta(x) = x(\bar{d} - \bar{u})$$
$$xS(x) = 2x(\bar{u} + \bar{d} + \bar{s})$$
$$xg(x)$$

- The total sea is made of, at Q^2_0 , $xu_{sea}(x)$, $xd_{sea}(x)$, $xs_{sea}(x)$ e $xc_{sea}(x)$:

$$xs_{sea} = 0.2S(x)$$
$$xu_{sea} = 0.4S(x) - 0.5c_{sea}(x) - x\Delta(x)$$
$$xd_{sea} = 0.4S(x) - 0.5c_{sea}(x) + x\Delta(x)$$

the symbol u_{sea}, d_{sea}, ... include the contribution from quarks and antiquarks to the sea.

Parton Distributions in the proton

- The 20% suppression of $xs_{sea}(x)$ comes from the data of events containing two muons in DIS events produced by neutrinos from the CCFR experiment.
- $xc_{sea}(x)$ (as also $xb_{sea}(x)$) is dynamically created with a correct treatment from Q^2 values near the threshold of production up to high Q^2.
- **Not all the p_i parameters are free** but:
  - p_1 for xu_v, xd_v are fixed by the sum rules, p_1 for xg by the rule for the momenta sum; $p_4 = 0$ for xg
  - p_2 is placed equal for xu_v and xd_v ;
  - for $x\Delta$: only p_1 is the free parameter fixed , while the shape of $x\Delta$ has to consistent with the Drell-Yan data. The value of p_1 was found compatible with the measured value of the Gottfried sum rule:

$$I_G = \int_0^1 \frac{dx}{x}\left(F_2^{\mu p} - F_2^{\mu n}\right) = \frac{1}{3}\int_0^1 dx\left(u_V - d_V + \bar{u} - \bar{d}\right) = \frac{1}{3} + \int_0^1 dx\left(\bar{u} - \bar{d}\right)$$

Parton Distributions in the proton

- Therefore there are only 11 free parameters in the fit, when α_s is fixed to $\alpha_s(M_Z) = 0.118$
- They are 12 if α_s remains free, not fixed
- The evolution of the equation is made at NLO in the MS-bar schema, the factorization and renormalization scales are chosen to be equal to Q^2.
- The value of Q^2_0 is 7 GeV^2
- $\alpha_s(Q^2)$ is calculated at two loops

- **Cuts applied to all the analyzed data:**
  - $Q^2 > 2.5$ GeV^2 : to remain in a region where pQCD should work
  - $W^2 > 20$ GeV^2: to reduce the dependence on higher-twist terms, sizable at low W^2
- The kinematical interval covered by the input data used in the fits is: $6.3 \cdot 10^{-5} \leq x \leq 0.65$, $2.5 \leq Q^2 \leq 30000$ GeV^2

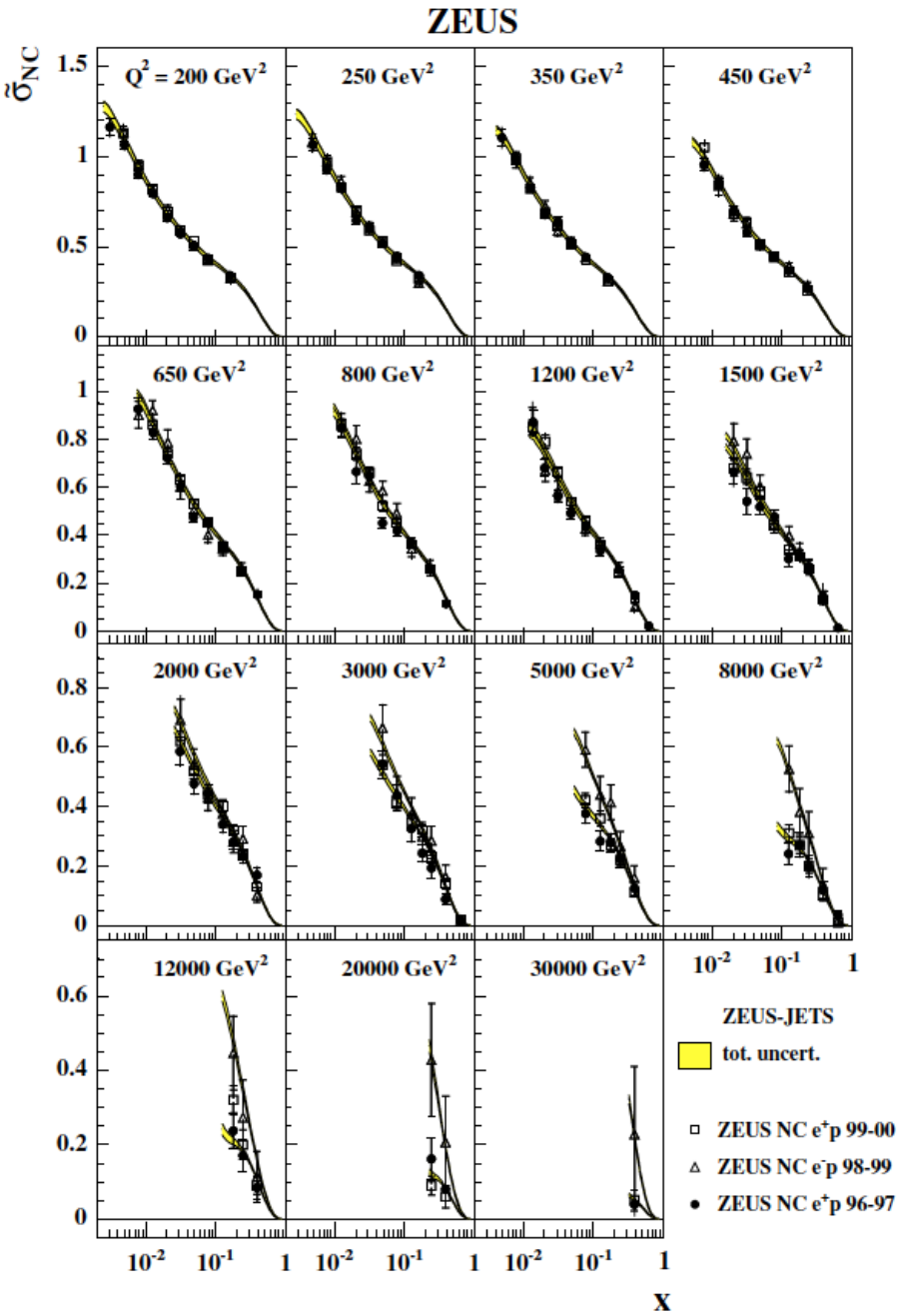

The fit gives an excellent description of the data

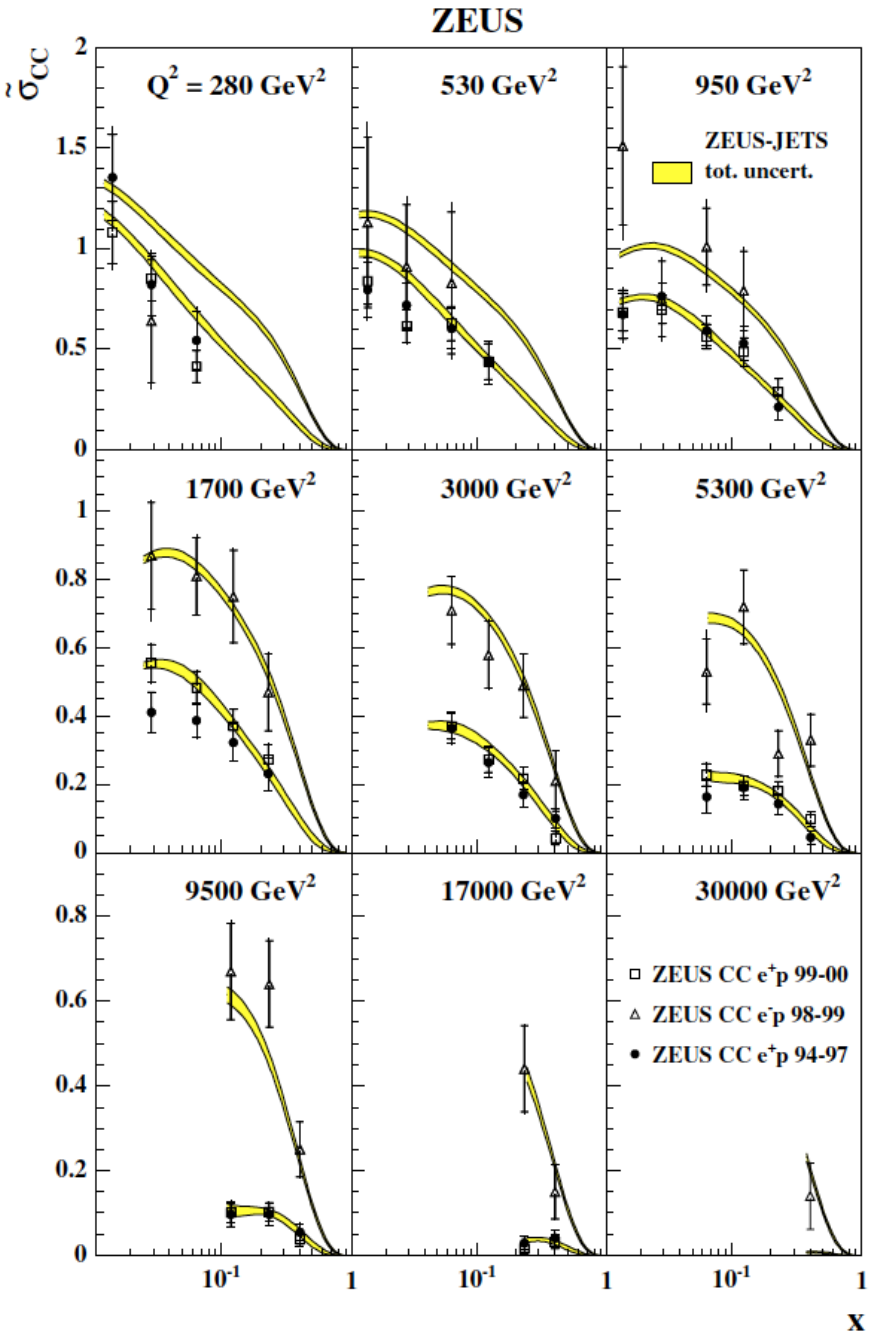

The fit gives an excellent description of the data

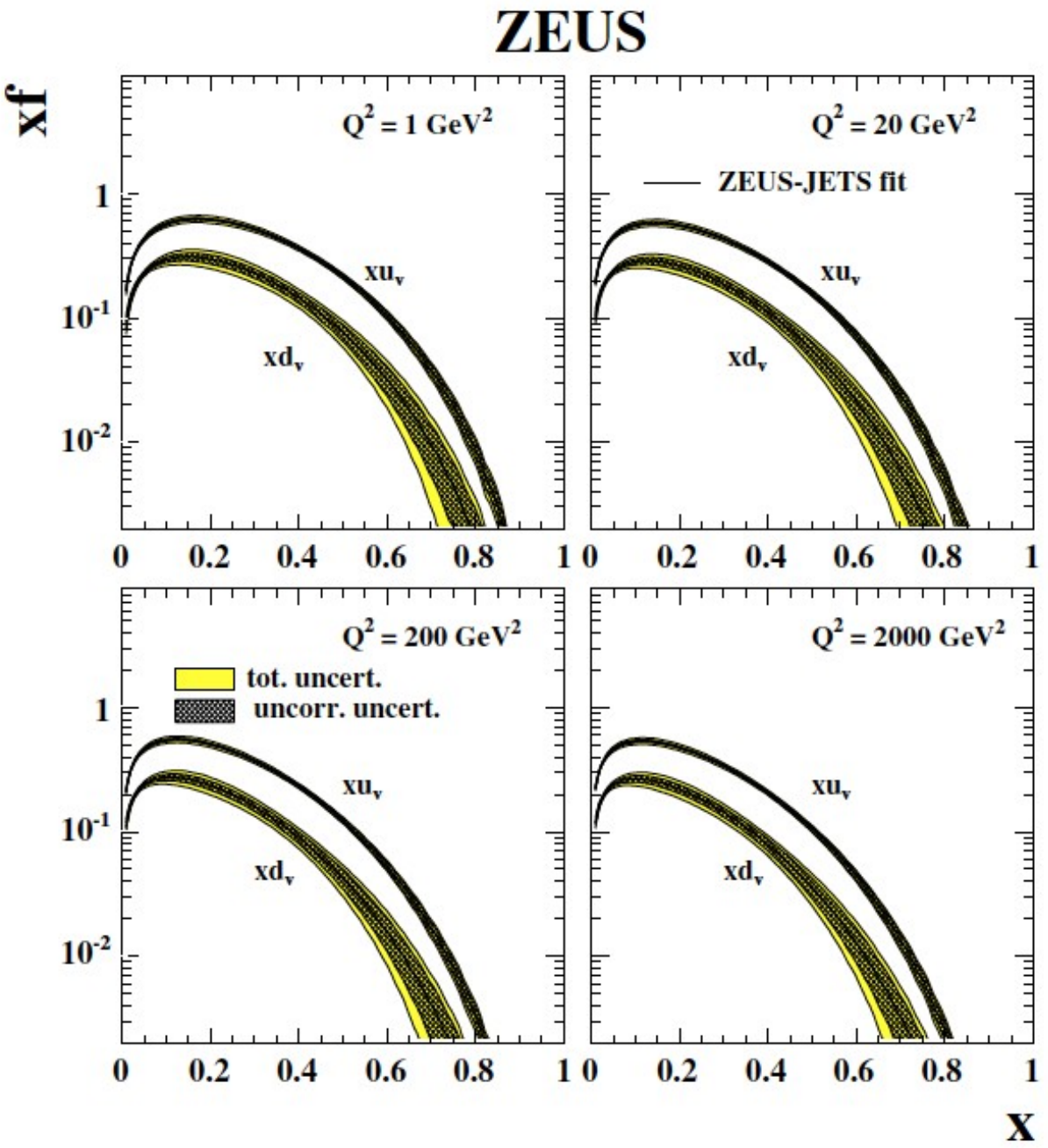

Valence quarks

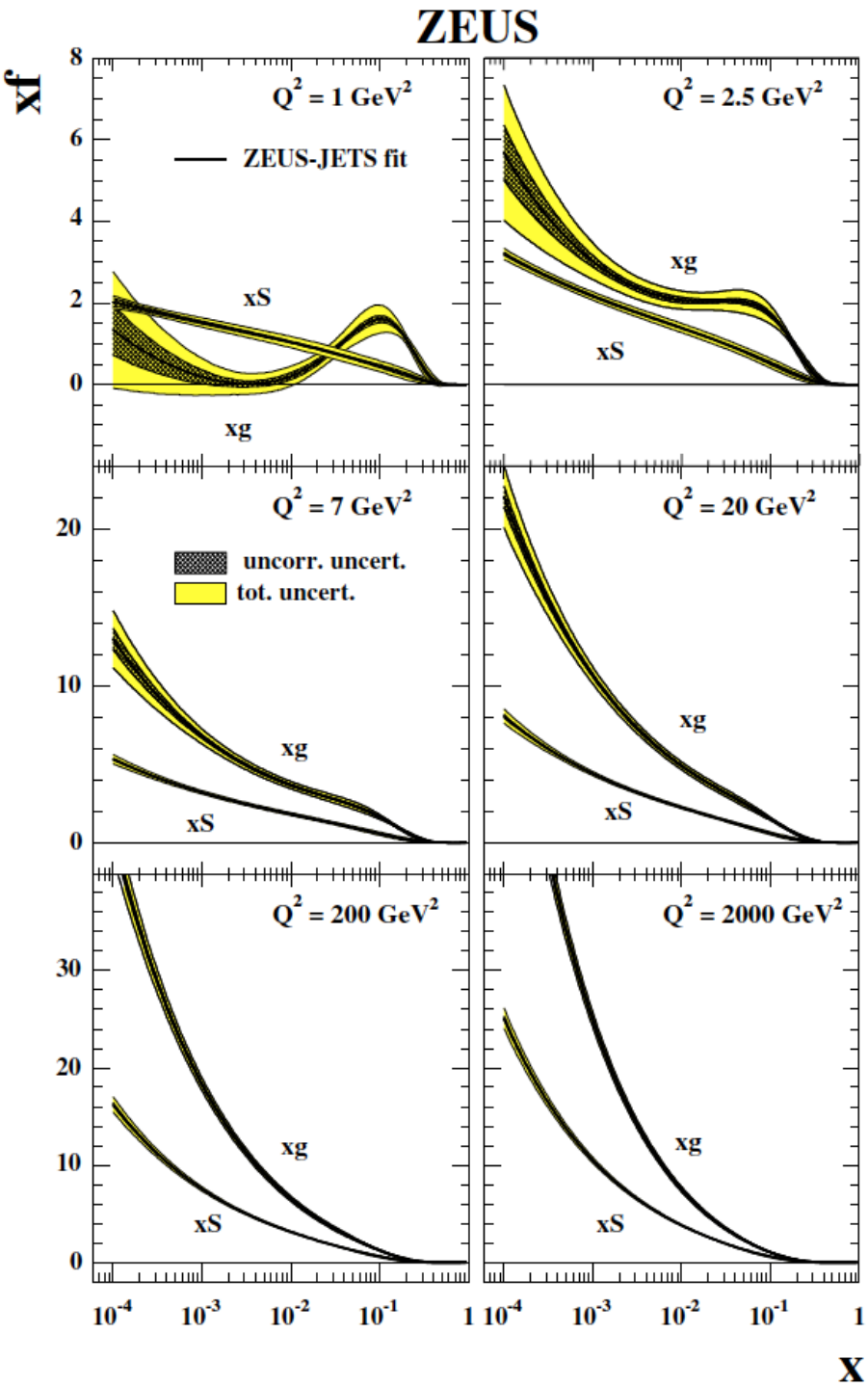

p.d.f. for the sea quaks and gluons

The sea p.d.f. increases at low *x* for all Q^2

The p.d.f. of the gluons flattens at Q^2 ~ 2.5 GeV^2, and becomes valence-like for lower Q^2

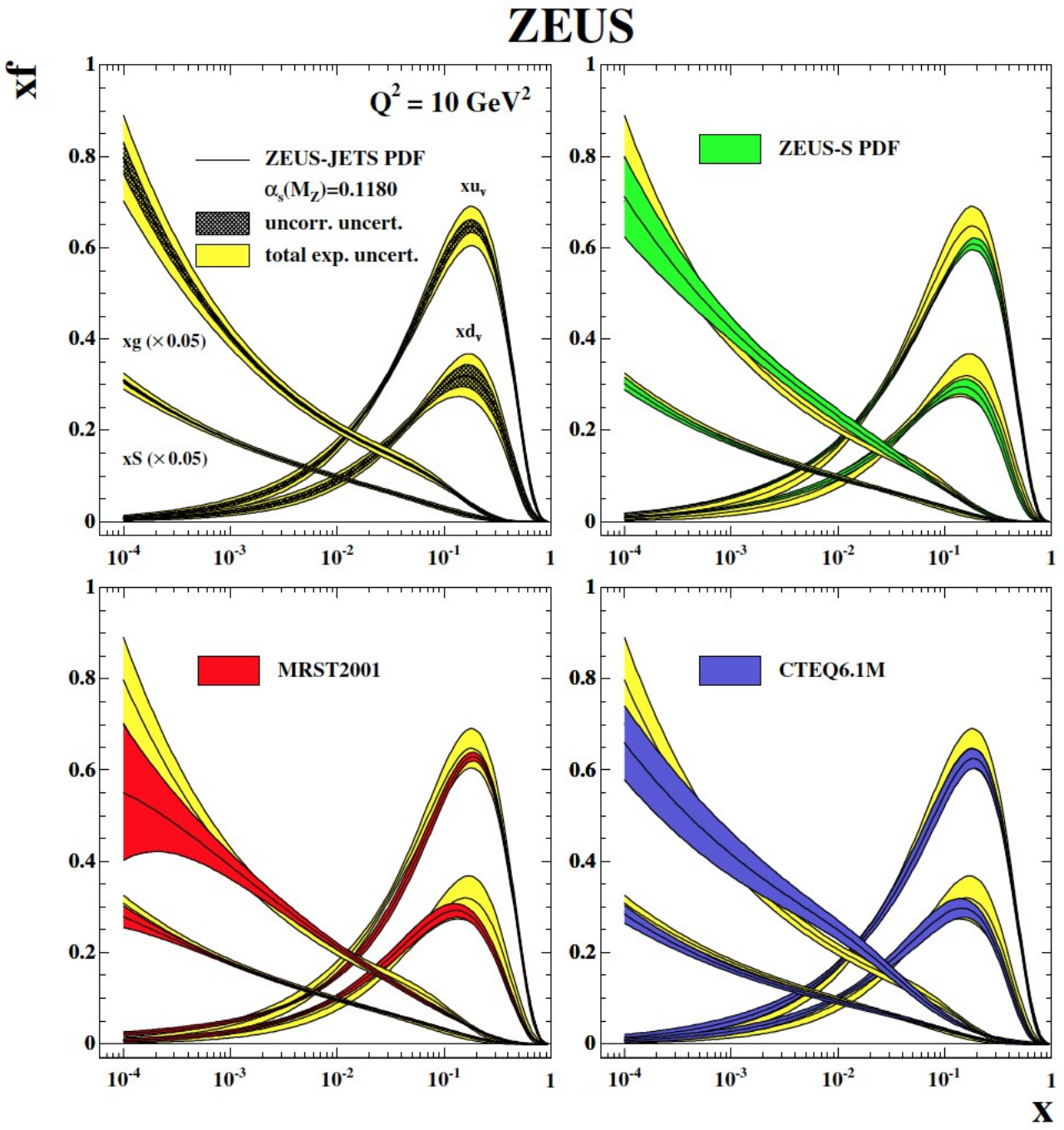

Comparison with other parameterizations

Fig. 7 Comparison of the parton distribution functions xu_v, xd_v, xg and $xS = x(\bar{U} + \bar{D})$ of HERAPDF2.0Jets NNLO with HERAPDF2.0 NNLO based on inclusive data only, both with fixed $\alpha_s(M_Z^2) = 0.118$, at the scale $\mu_f^2 = 10\,\mathrm{GeV}^2$. The uncertainties of HERAPDF2.0Jets NNLO are shown as differently shaded bands and the central value of HERAPDF2.0 NNLO is shown as a dotted line

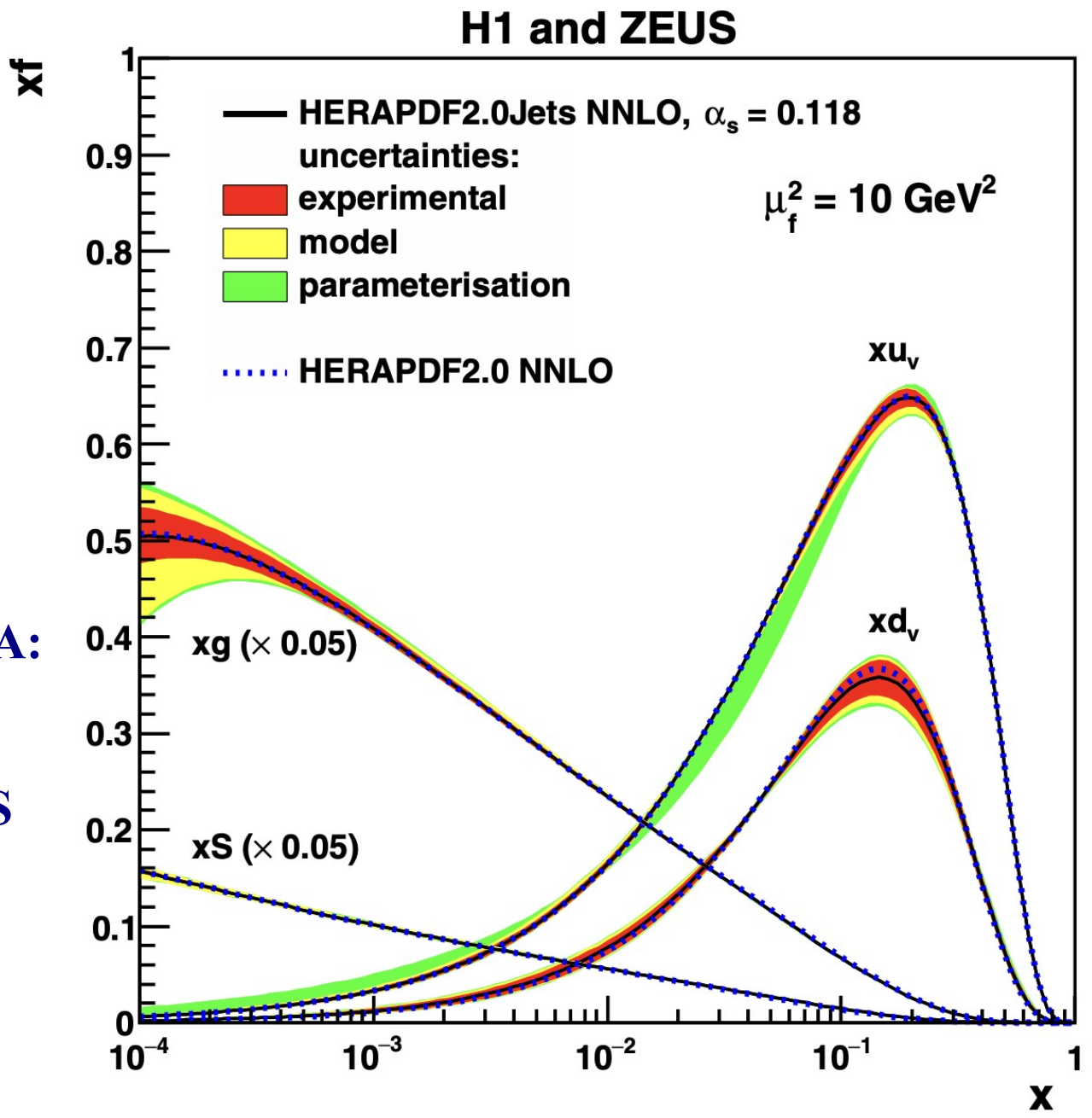

Final results from HERA: combination of all inclusive data and jets data from H1 and ZEUS experiments
Measurements made at NNLO

New developments

Process	Subprocess	Partons	x range
$\ell^\pm\{p,n\} \to \ell^\pm X$	$\gamma^* q \to q$	$q, \bar{q}, g$	$x \gtrsim 0.01$
$\ell^\pm n/p \to \ell^\pm X$	$\gamma^* d/u \to d/u$	d/u	$x \gtrsim 0.01$
$pp \to \mu^+\mu^- X$	$u\bar{u}, d\bar{d} \to \gamma^*$	$\bar{q}$	$0.015 \lesssim x \lesssim 0.35$
$pn/pp \to \mu^+\mu^- X$	$(u\bar{d})/(u\bar{u}) \to \gamma^*$	$\bar{d}/\bar{u}$	$0.015 \lesssim x \lesssim 0.35$
$\nu(\bar{\nu})\, N \to \mu^-(\mu^+)\, X$	$W^* q \to q'$	$q, \bar{q}$	$0.01 \lesssim x \lesssim 0.5$
$\nu\, N \to \mu^-\mu^+ X$	$W^* s \to c$	s	$0.01 \lesssim x \lesssim 0.2$
$\bar{\nu}\, N \to \mu^+\mu^- X$	$W^* \bar{s} \to \bar{c}$	$\bar{s}$	$0.01 \lesssim x \lesssim 0.2$
$e^\pm p \to e^\pm X$	$\gamma^* q \to q$	$g, q, \bar{q}$	$10^{-4} \lesssim x \lesssim 0.1$
$e^+ p \to \bar{\nu} X$	$W^+\{d,s\} \to \{u,c\}$	d, s	$x \gtrsim 0.01$
$e^\pm p \to e^\pm c\bar{c}X, e^\pm b\bar{b}X$	$\gamma^* c \to c$, $\gamma^* g \to c\bar{c}$	c, b, g	$10^{-4} \lesssim x \lesssim 0.01$
$e^\pm p \to$ jet$+X$	$\gamma^* g \to q\bar{q}$	g	$0.01 \lesssim x \lesssim 0.1$
$p\bar{p}, pp \to$ jet(dijet)$+X$	$gg, qg, qq \to 2j$	g, q	$0.00005 \lesssim x \lesssim 0.5$
$p\bar{p} \to (W^\pm \to \ell^\pm\nu)\, X$	$u\bar{d} \to W^+, \bar{u}d \to W^-$	$u, d, s, \bar{u}, \bar{d}, \bar{s}$	$x \gtrsim 0.05$
$pp \to (W^\pm \to \ell^\pm\nu)\, X$	$u\bar{d} \to W^+, d\bar{u} \to W^-$	$u, d, s, \bar{u}, \bar{d}, \bar{s}, g$	$x \gtrsim 0.001$
$p\bar{p}(pp) \to (Z \to \ell^+\ell^-)X$	$uu, dd, ..(u\bar{u}, ..) \to Z$	$u, d, s, ..(g)$	$x \gtrsim 0.001$
$pp \to W^- c,\ W^+\bar{c}$	$gs \to W^- c$	$s, \bar{s}$	$x \sim 0.01$
$pp \to (\gamma^* \to \ell^+\ell^-)X$	$u\bar{u}, d\bar{d}, .. \to \gamma^*$	$\bar{q}, g$	$x \gtrsim 10^{-5}$
$pp \to (\gamma^* \to \ell^+\ell^-)X$	$u\gamma, d\gamma, .. \to \gamma^*$	γ	$x \gtrsim 10^{-2}$
$pp \to b\bar{b}\, X,\quad t\bar{t}X$	$gg \to b\bar{b},\quad t\bar{t}$	g	$x \gtrsim 10^{-5}, 10^{-2}$
$pp \to t(\bar{t})\, X,$	$bu(\bar{b}d) \to td(\bar{t}u)$	$b, d/u$	$x \gtrsim 10^{-2}$
$pp \to$ exclusive $J/\psi, \Upsilon$	$\gamma^*(gg) \to J/\psi, \Upsilon$	g	$x \gtrsim 10^{-5}, 10^{-4}$
$pp \to \gamma\, X$	$gq \to \gamma q,\ g\bar{q} \to \gamma\bar{q}$	g	$x \gtrsim 0.005$

fixed target experiments

HERA experiments

***pp̄* Tevatron/ *pp* LHC**

New developments

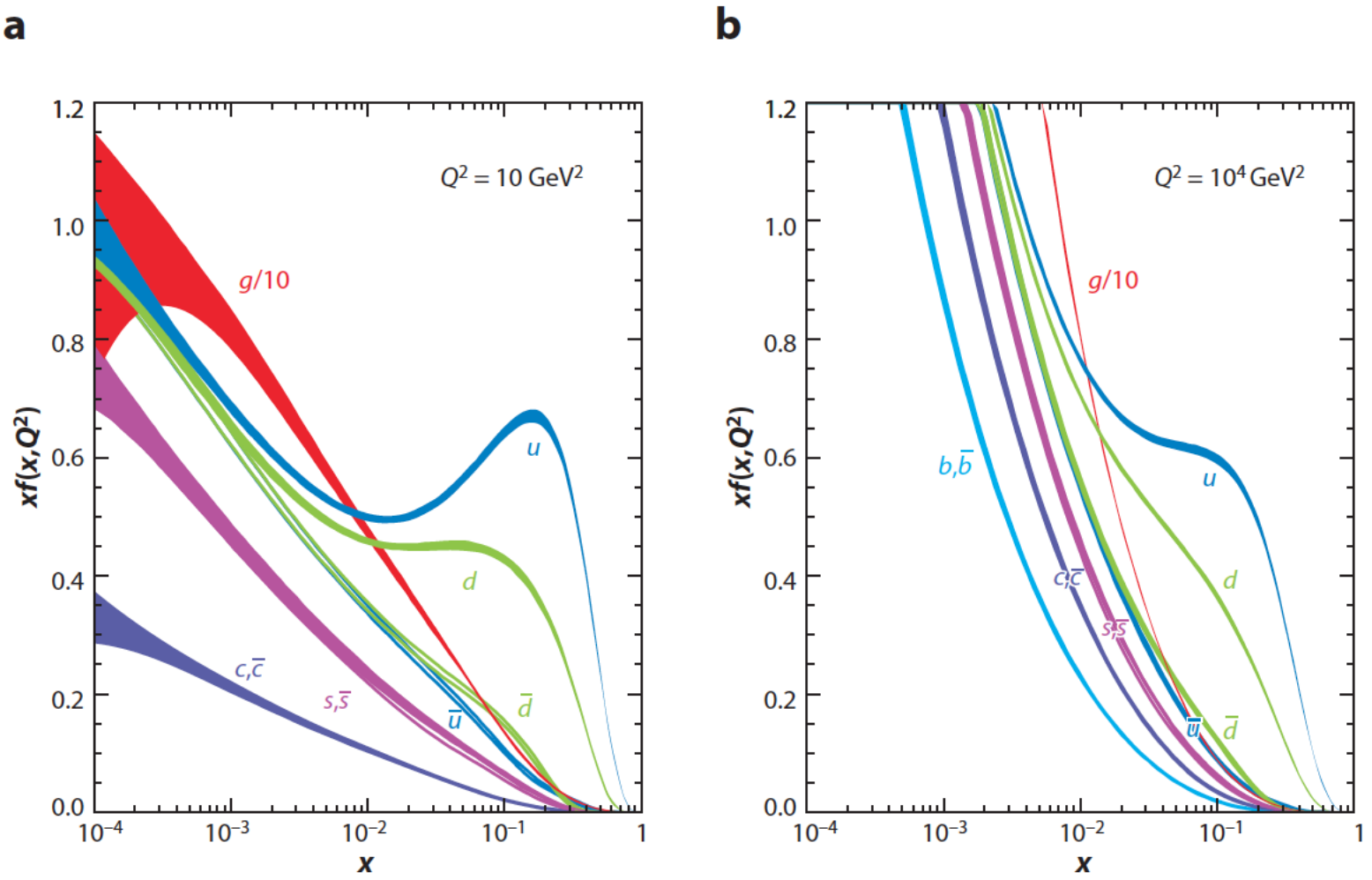

Figure 3

MSTW08 (27) next-to-next-to-leading-order parton distribution functions at (*a*) $Q^2 = 10$ GeV^2 and (*b*) $Q^2 = 10^4$ GeV^2.